Development of genetic tools in environmental *Pseudomonas* species

A THESIS
SUBMITTED TO THE FACULTY OF THE
UNIVERSITY OF MINNESOTA
BY

Madison Jordan Kalb

IN PARTIAL FULFILLMENT OF THE REQUIREMENTS
FOR THE DEGREE OF
MASTER OF SCIENCE

Advisor: Jeffrey A. Gralnick

December 2022

ACKNOWLEDGEMENTS

The work presented in this thesis would not have been completed without the support of many people. To my mentor and advisor, Jeffrey Gralnick, I want to thank you for all of your support over the past 2 years. I am so grateful to you for introducing me to the world of bacterial genetics and your incredible trust in me to work on bunch of new bugs in your lab.

I would also like to thank my committee for their gracious support and feedback on my research: Katie Fixen, Kyle Costa, and Jeffrey Gralnick. An additional shout-out goes out to Daniel Bond, whose questions after my various lab presentations always gave me new considerations to mull over.

To my fellow present and past Gralnick and Bond lab members, thank you all very much for your support during my time at UMN. I'll forever be reminded of you all whenever I eat a bagel or play a game of "hang-man". A special thanks goes out to my dear friend and mentor Abhiney Jain, for both your emotional and intellectual support. To Sol Choi, your positive energy and support have always put a smile on my face, which I especially needed during this process. A big thank you also goes out to David Hsu for being my writing buddy and hype-man. To my dear undergrad Jane Fenske-Newbart, you will always hold a special place in my heart as my first mentee; thank you for always being my second set of hands. I am honored to have been able to teach you what I know about science, and I cannot wait to see what your future holds.

To my friends and family, I cannot begin to express how much I appreciate your love and support in completing this work.

Dedication

This thesis is dedicated to my mom, who I know would have been really proud.

Abstract

Plant growth-promoting rhizobacteria possess many beneficial traits that make them desirable in agricultural applications. Several *Pseudomonas* spp. have developed a close association with plants and perform nutrient exchange as well as protect the plant from pathogens. Limited research has been done in genetically manipulating these organisms, which could further enhance the agricultural utility of these strains, providing a far less destructive alternative than the chemical fertilizers and pesticides used today. In this work I aimed to build a genetics system in several species of environmental *Pseudomonas* as the basis for future manipulation and research within these strains. I first investigated growth dynamics and transformation strategies to later introduce phage-derived recombinases for directed chromosomal mutation of the *rpoB* gene while providing direct comparison of these criteria between different strains of *Pseudomonas.* I also highlight some of the unique behavior within these *Pseudomonas* spp. that further emphasizes the individuality between strains and difficulty in creating a "one-size fits all" protocol, while identifying key components to consider when adapting an environmental bacterium to life in the lab.

TABLE OF CONTENTS

LIST OF TABLES

LIST OF FIGURES

Chapter 1: Building a genetics system in environmentally derived *Pseudomonas spp.*

1.1 Abstract

As the world population continues to grow, our current ability to adapt to the needs of our society have struggled to maintain a comparable pace. Our current methods of food, product, and energy production have created the conditions which have led to toxic chemical buildup, high pollution emissions, and extinction events around the world. Some bacteria possess valuable qualities that may provide potential solutions to these problems in bioremedial or sustainable product applications. One such group of bacteria are plant growth-promoting rhizobacteria (PGPR), which enhance the growth of many plants, including relevant agricultural crops through several mechanisms. *Pseudomonas* has many plant growth-promoting strains, 8 of which are investigated to various extents in this study. Here I inspect several key aspects to building genetics systems in these *Pseudomonas* strains, which allow for the future development of robust studies within these strains.

1.2 Rationale of interest

Environmentally-derived bacteria possess many attractive qualities when considering potential industrial, agricultural, or pharmaceutical applications—one of which being they are generally more robust and stress-tolerant compared to laboratory domesticated strains due to the harsher growth conditions they have evolved to endure. These harsher and more competitive native habitats of "wild" bacteria generate diverse metabolic capabilities as each species finds their respective niche to survive. For some bacteria, like *Prochlorococcus* spp. or *Mariprofundus* sp., this involves becoming a metabolic specialist and utilizing metals in the environment as a means for respiration (1, 2). Other bacteria, like *Pseudomonas* spp. survive in a variety of environments due to their metabolic versatility, which allows them to compete against other bacteria under fluctuating nutrient identity and availability.

Rhizobacterial *Pseudomonas* spp., have evolved to develop complex secondary metabolisms to produce compounds with a layered purpose: to directly promote plant growth by

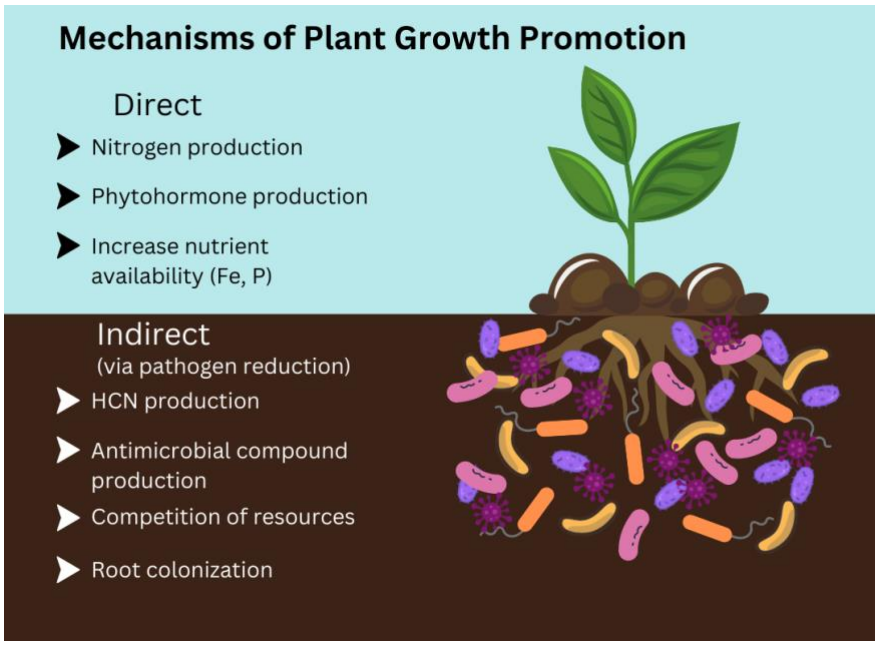

Figure 1.1. Mechanisms of Plant Growth Promotion in *Pseudomonas*. Overview of the direct and indirect mechanisms utilized by rhizobacterial *Pseudomonas* spp. to improve host plant performance.

producing phytohormones to influence plant behavior or increasing nutrient availability in the soil, or to indirectly improve growth conditions by reduce competition with other microbes, including bacterial and fungal pathogens (3-5) (Figure 1.1). Furthermore, rhizobacterial *Pseudomonas* spp. are well able to colonize the rhizosphere due to their quorum sensing and biofilm forming capabilities, which allows them to benefit from C and N nutrient exchange on root exudates (4-9). Because of these properties, several environmental *Pseudomonas* spp. have been identified with promising potential as agriculturally relevant biocontrol strains, including *P. protegens* Pf-5, *P. protegens* CHA0, *P. fluorescens* Pf-01, *P. ogarae* F113, *P. fluorescens* SBW25, *P. chlororaphis* 30-84, and *P. putida* KT2440. Though these bacterial strains are considered as promising candidates in this area, relatively little genetic manipulation has been performed in these strains to further optimize these properties and generate genetically engineered microbes (GEMs) that would have commercial value as biopesticides. This work aims to act as a guide for ground-up domestication of environmental Pseudomonads in implementing a genetics system, which could be loosely applied to colony-forming Gammaproteobacteria, as well as an overview in how strain diversity itself leads to variable performance under genetically identical systems.

1.3 Plant growth-promoting rhizobacteria potential in agriculture

As the world population continues to grow, the demand placed on our food chain does as well; therefore, the need to develop sustainable agricultural practices is of the utmost importance. It is anticipated that by 2067 the maximal estimated food production levels based on amount of available arable land and fertilizers will be exceeded by global food demand (10). The main limiting factor in current crop yields is biological in the forms of pests, weeds, and disease, which is estimated to cause between 27 and 42% of crop loss annually (11). For most of the 20th century, the main additives to improve crop yield based on biological controls were in the form of chemical pesticides and fertilizers. These methods have various negative impacts on the environment including the development of pesticide resistance, chemical residues present in harvested foods, degradation of soil health, and eutrophication of aquatic ecosystems due to nitrogen and phosphorus runoff (5, 10, 11). The idea of "biopesticides" in the forms of plant-associated microbes or microbially-derived metabolites have become increasingly popular as they can both stimulate plant growth and act as biocontrol agents against pathogenic species and pests (12). Plant growth-promoting rhizobacteria (PGPR) are a group of bacteria that closely associate with the plant rhizosphere and have many beneficial effects on plant health. These organisms, when applied to crops as biopesticides, are also less detrimental on soil health and natural ecology (5). Species from several genera have been toted for their potential as commercially relevant PGPR, including *Bacillus, Streptomyces, Azospirillum, Burkholderia, Azotobacter, Serratia* and *Pseudomonas* (5, 8, 12). Further development of these PGPR strains using genetic tools is vital to the application of PGPR as the next frontier of bio-based fertilizers and pesticides.

1.4 Diversity of environmental Pseudomonas and plant growth-promoting properties

Pseudomonas is a well-known genus of bacteria, recognized most infamously from the species *P. aeruginosa* and *P. syringae*, human and plant pathogens, respectively, whose detrimental impacts on human society ultimately fueled interest in the genus (13). The diverse metabolic capability within the genus was recognized early during the 20th century, leading to the assignment of many other species including betaproteobacteria *Ralstonia, Bulkholderia*, and *Comomonas* as well as alphaproteobacteria *Methylobacterium* and *Sphingomonas* to

Pseudomonas (4, 13, 14). RNA:DNA hybridization, 16S sequencing, and DNA:DNA hybridization restructured the taxonomy of the genus in the 1990s to what it is accepted as today—with the phenotype of aerobes, usually with polar flagella, that produce pigmented products like pyocyanin, fluorophores, or siderophores, and can metabolize a wide variety of organic compounds (13-15). The diverse metabolic capabilities of these organisms contribute to their abilities to both tolerate environmental fluctuations and inhabit a variety of environments, from aquatic to terrestrial. Many strains within the genus have developed a close association with plants—either pathogenic, like *P. syringae* and *P. ficusrectae,* or plant growth-promoting, like the strains investigated in this study: including *P. protegens* Pf-5, *P. protegens* CHA0, *P. fluorescens* Pf0-1, *P. ogarae* F113, *P. fluorescens* SBW25, *P. chlororaphis* 30-84, and *P. putida* KT2440. These strains have been isolated from various parts of the planet and have been shown to inhabit the rhizosphere of many plants including sugar beets, cotton, corn, tobacco, wheat, alfalfa, willow, pine, and rosemary, among others (3-5, 9, 16-21). The strains selected for this study span a variety of plant associations, plant growth-promoting properties, and have various degrees of relatedness: with strains *P. protegens* CHA0, *P. protegens* Pf-5, *P. fluorescens* Pf0-1, *P. ogarae* F113, *P. chlororaphis* 30-84, and *P. fluorescens* SBW25 representing 4 out of the 5 subgroups within the *P. fluorescens* group (20).

The plant growth-promoting properties of these strains primarily falls into three categories: reducing the burden of pathogens via the production of antibiotic-like secondary metabolites and hydrogen cyanide (HCN), increasing nutrient availability in the soil, or by stimulating plant behavior to encourage new growth or defensive mechanisms by phytohormone production (Figure 1.1). An overview of the distribution of these properties within each strain is in Table 1.1.

The antibiotic-like secondary metabolites produced by these *Pseudomonas* spp. include phenazines, phloroglucinols, pyoluteorin, pyrrolnitrin, rhizoxin, orfamides, and furanomycin (5). Phenazines are pigmented cyclic compounds that are broadly antimicrobial and antifungal and inhibit growth via accumulation of toxic superoxides and hydrogen peroxide. Phenazines phenazine-1-carboxylate (PCA) and phenazine-1-carboxamide (PCN) produced by various *Pseudomonas* spp. have been shown to inhibit growth of phytopathogens *Fusarium oxysporum*

Table 1.1. Overview of *Pseudomonas* spp. characteristics in this study.

Strain	Genome Size (Mbp)	# predicted genes	G+C content (%)	Isolation	Plant growth-promoting properties/secondary metabolites produced
P. protegens Pf-5 (formerly *P. fluorescens* Pf-5)	7.1 (25)	6,3117 (25)	63 (25)	Cotton seedling rhizosphere, 1978 (USA) (17)	PCA, orfamides (26), pyoverdine (25), pyoluteorin (27), 2,4-diacetylphloroglucinol (28), rhizoxin (29), HCN (25), pyrrolnitrin (17, 30), enantio-pyochelin (31)
P. protegens CHA0 (Formerly *P. fluorescens* CHA0)	6.9 (32, 33)	6,260 (32)	63.4 (32, 33)	Tobacco roots, 1983 (Switzerland) (34)	Pyoverdine (35), pyoluteorin (27), 2,4 diacetylphloroglucinol (36), HCN (37), enantio-pyochelin (6)
P. ogarae F113 (Formerly *P. fluorescens* F113)	6.8 (20, 38)	6,154 (20, 38)	60.8 (20, 38)	Sugar beet rhizosphere, 1992 (UK) (16)	2,4-diacetylphloroglucinol (16), pyoverdine (39), phosphate solubilization (40), HCN (41), pyridine-2,6-bis-thiocarboxylic acid (42), denitrification* (20, 38)
P. fluorescens Pf0-1	6.4 (43)	5,870 (43)	60.5 (43)	Loam soil, 1988 (USA) (44)	Pyoverdine (45), phosphate solubilization (46)
P. fluorescens SBW25	6.7 (43)	6,009 (43)	60.5 (43)	Sugar beet leaf, 1989 (UK) (47)	Pyoverdine (48), viscosin-like cyclic lipopeptide (49), furanomycin (50)
P. chlororaphis subsp. aureofaciens 30-84 (Formerly P. aureofaciens 30-84)	6.7 (51)	6,020 (51)	62.5 (51)	Wheat rhizosphere, 1979 (USA) (52)	PCA (22, 24), 2-OH-PCA (53), 2-OH-phenazine (24), pyrrolnitrin (54), phytohormone production* (54).
P. putida KT2440 (Formerly *P. aravilla mt-2)*(55)	6.2 (56)	5,691 (57)	61.5 (56)	Cultivated field, 1961 (Japan) (58)	Pyoverdine (45), phosphate solubilization (59), phytohormone production* (60), organic pollutant degradation* (57), salinity tolerance (60)
P. synxantha 2-79 (Formerly *P. fluorescens* 2-79)	6.4 (62)	5,674 (62)	59.8 (62)	Wheat rhizosphere, 1979 (USA) (52)	PCA (24,63), pyoverdine (64), HCN synthesis* (62), anthranilic acid (65)

Genome size, number of predicted genes, and G+C content for each strain was determined using the most recently updated genome assemblies available on NCBI. Plant growth-promoting properties solely supported by in silico data are denoted by "*".

sp., *Gaeumannomyces graminis* var. tritici, *Phythium* sp*., Bacillus subtiliis*, *Erwinia amylovora*, *and Actinomyces viscosus* (22-24). The phloroglucinol 2,4 diacetylphloroglucinol is highly toxic due to its impact on mitochondrial functioning and calcium homeostasis and is effective against nematodes, bacteria, fungi, and protists (66, 67). Its production is widely distributed in the *P. fluorescens* group (5). The antibiotic pyoluteorin is effective against fungal pathogens *Botrytis cinereal* and *Heterobasidion* spp.as well as the oocyte *Pythium ultimum* (27, 68, 69). Pyrrolnitrin is an antifungal compound effective against *Rhizoctomium solani, Deuteromycete*, *Ascomycete,* and *Basidiomycete* (17). Rhizoxin, found in *P. protegens* Pf-5, is effective against fungi *Botrytis cinereal*, oomycete *Phytophthora ramorum,* and insect *Drosophila melanogaster* (29, 70), while orfamides, also found in *P. protegens* Pf-5, have the ability to lyse zoospores of *P. ramorum*. The antibiotic furanomycin, originally only thought to be produced by *Streptomyces* spp*.,* is produced by *P. fluorescens* SBW25 (50). It is effective against a wide variety of bacterial plant pathogens including *D. dadantii* and *P. syringae* by competitively inhibiting isoleucine, affecting protein translation (50, 71). Production of HCN is also provides protection to associated plants by inhibiting cytochrome c oxidase, suppressing fungal pathogens like *P. ultimum* and *F. oxysporum* (72).

Siderophores are a large family of metal scavenging compounds that are produced by many Pseudomonads (6). They primarily are secreted into the environment under iron limiting conditions and are selectively brought back into the cell by surface membrane transporters that recognize the chelated form of these compounds. Pseudomonads typically produce a primary siderophore, pyoverdine, as well as a secondary siderophore, which can perform iron scavenging as well but has a lower affinity for iron, like pyochelin, enantio-pyochelin and pseudomonin (6). Pyoverdines are fluorescent compounds responsible for the fluorescence of many *Pseudomonas* species. They consist of an identical chromophore, an organic acid or amide side chain, and a strain specific peptide group so the only chelated pyoverdines that can be imported is the one it produces or one very structurally similar (6). Pyoverdine can also scavenge other environmental metals nickel, cadmium, and copper, although to a lesser degree. Secondary siderophores function similarly to pyoverdine but are usually secreted under conditions where iron is less scarce (6). The siderophores promote plant growth by competitively reducing iron availability for pathogenic bacteria and fungi, as well supporting iron uptake by the plant through nutrient exchange (3, 8).

Some *Pseudomonas* spp. investigated in this study also promote plant growth by enhancing phosphate availability. After nitrogen, phosphorus is the second highest nutrient required for plant growth. 99% of environmental phosphate is found in insoluble forms, which plants cannot easily utilize (3). Secretion of organic acids like gluconic acid, citrate, lactate, and succinate solubilize the inorganic phosphate into soluble $H_2PO_4^-$ or HPO_4^{2-} ions which can be absorbed by the plant (8). Phosphate can also be made available to plants via microbial secretion of phosphatases (3). Genomic evidence for phosphate availability via phosphatase secretion is found in strains *P. fluorescens* Pf0-1 and *P. ogarae* F113 by presence of genes *phoD* and *phoX* (20, 45), which was further supported by in vitro studies in *P. fluorescens* Pf0-1.

P. putida KT2440 and *P. chlororaphis* 30-84 have been reported to produce phytohormones, small molecules that influence plant physiological processes. Genes encoding 1-aminocyclopropane-1-carboxylate (ACC) deaminase are present in the *P. chlororaphis* 30-84 genome. ACC deaminase degrades ethylene buildup to enhance root growth (54). Furthermore, production of an antimicrobial plant auxin phenylacetic acid (PAA) is also supported by a gene cluster found in the *P. chlororaphis* 30-84 genome (54, 73). A synthesis pathway for the well-known phytohormone indole-3-acetic-acid (IAA) is found in *P. putida* KT2440 (60). IAA is responsible for regulating many growth responses within a plant, including fruit production, root elongation, and cell division (5, 74).

1.5 Results

After first isolating a new bacterium or working with an unfamiliar strain of bacteria, several logical steps must first be completed in order to develop a genetics system within that host. This section highlights those steps and how they were implemented in our panel of *Pseudomonas* isolates. This includes testing growth media, determining appropriate minimum inhibitory concentrations (MICs) of various antibiotics for the strain, establishing how to transform DNA into the bacteria, testing compatible origins of replication (oriCs), and finetuning inducible systems for controlling levels of gene expression.

Growth rate comparison in different rich media

The effect of rich media on growth rates was compared in a subset of the *Pseudomonas* strains using Lysogeny Broth (LB) and King's B medium (Figure 2). In all strains except *P. fluorescens*

Pf0-1, LB media supported faster growth rates. The effect of media on growth rate was minimal in *P. ogarae* F113, with each medium supporting similar doubling times, while the growth rates in *P. synxantha* 2-79 and *P. chlororaphis* 30-84 grew much faster in LB when compared to King's B medium. In all strains except *P. protegens* Pf-5, a higher final OD_{600} was observed when cultured in King's B medium compared to LB.

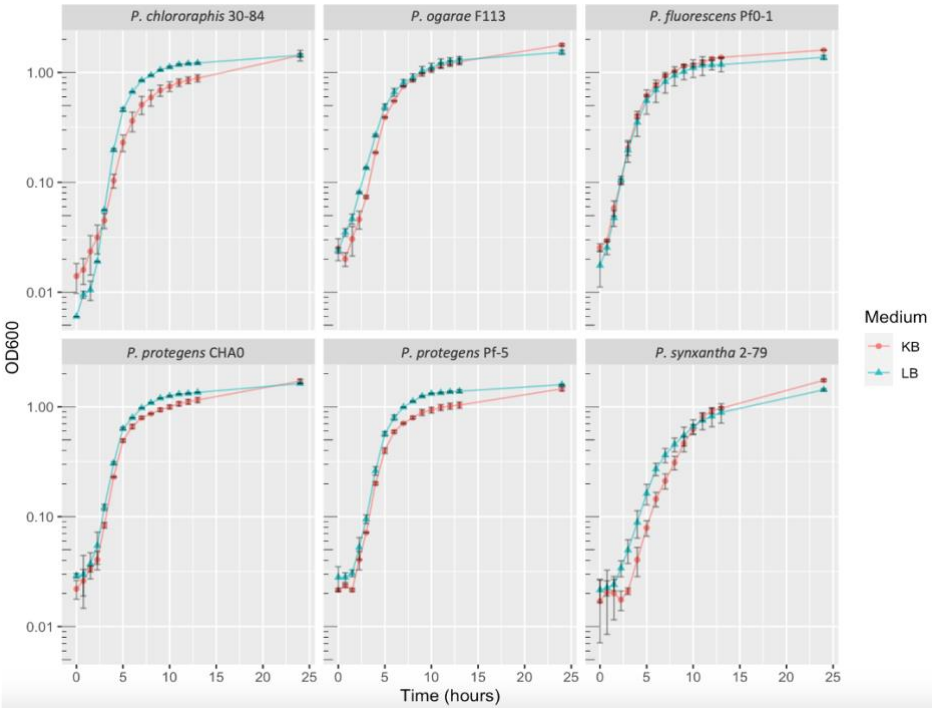

Figure 1.2. Growth curves of *Pseudomonas* spp. in different rich media. OD_{600} of *Pseudomonas* spp. cultures was monitored over a 24-hour period to measure growth rate. Results from single experiment using 2 biological replicates.

Determining MICs in *Pseudomonas* isolates

A selection of 6 bacteriostatic or bactericidal antibiotics with various cellular targets were tested at different concentrations in liquid culture to determine MICs for each strain (Figure 1.3). The bacteriostatic antibiotics chosen were chloramphenicol, which binds to the 50S ribosomal subunit, and tetracycline, which binds to the 30S ribosomal subunit, preventing transcription in each case (75, 76). The bactericidal antibiotics chosen were ampicillin, a beta-lactam antibiotic that affects peptidoglycan synthesis, and aminoglycoside antibiotics kanamycin, gentamicin, and streptomycin, which irreversibly bind to the 30S ribosomal subunit and 4 nucleotides of 16S rRNA (77-80).

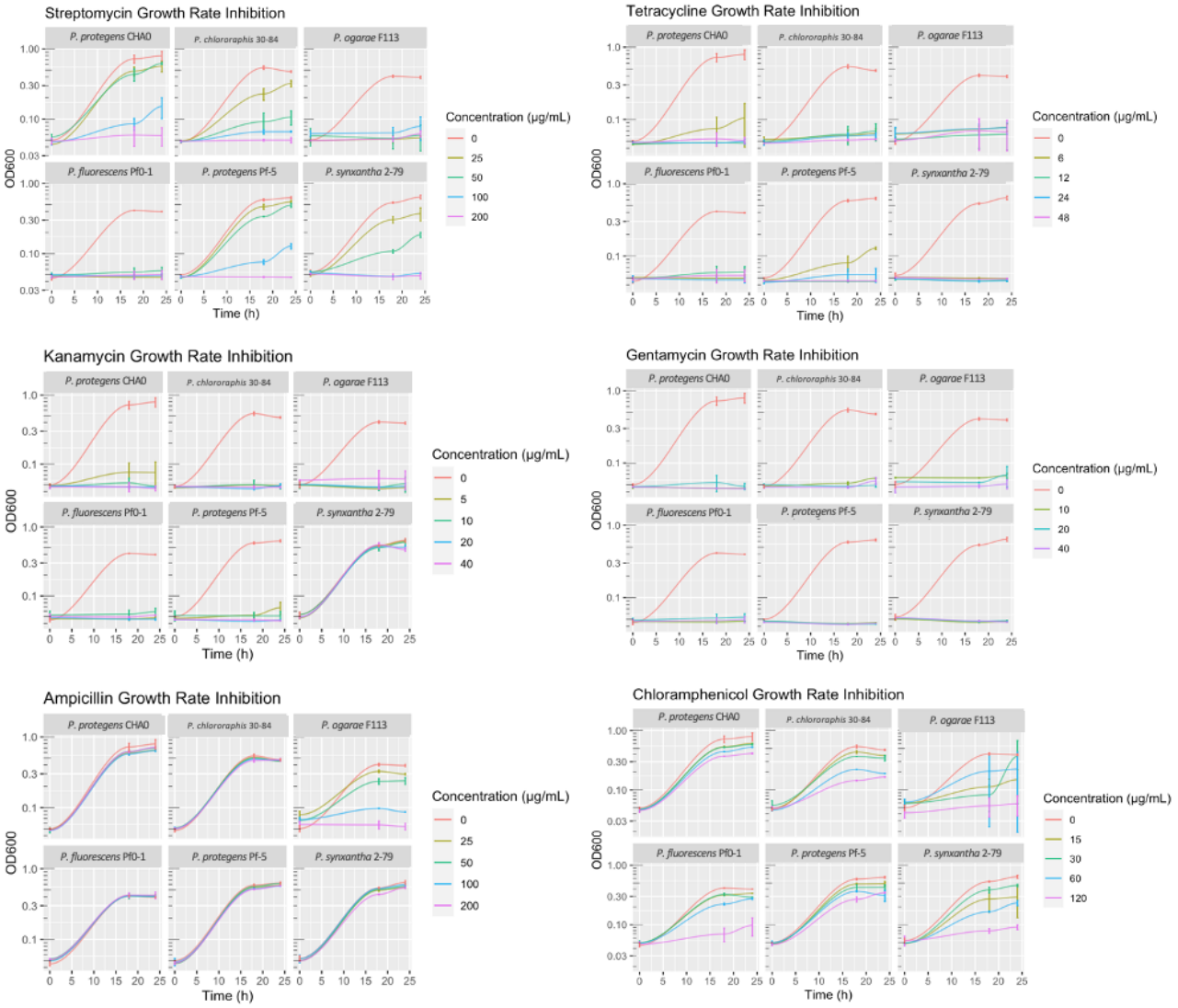

Figure 1.3. Effect of different antibiotics on growth of *Pseudomonas* spp. OD_{600} of different *Pseudomonas* strains when treated at different concentrations of 6 antibiotics. Results of single experiment with biological replicates for each strain and concentration.

Each strain exhibited variable response to the antibiotics tested, but in general were sensitive to gentamicin, tetracycline, and kanamycin. *P. synxantha* 2-79, however, was notably very resistant to kanamycin and exhibited no growth defect at the highest concentration tested, 200 µg/mL. Tetracycline treatment inhibited growth in all strains at concentrations above 12 µg/mL. Gentamicin was effective at low concentrations of 10 µg/mL in all strains. All strains except the *P. fluorescens* group strains (Pf0-1 and F113) showed a concentration-dependent growth inhibition when treated with streptomycin—these strains were inhibited at the lowest concentration tested, 25 µg/mL. Chloramphenicol exhibited dose-dependent growth inhibition in

all strains but was least effective in growth prevention in the *P. protegens* strains (Pf-5 and CHA0). Interestingly, *P. ogarae* F113 was the only strain sensitive to the beta-lactam antibiotic ampicillin.

Using this information, the three most widely effective antibiotics, kanamycin, gentamicin, and tetracycline, were further tested with each strain via agar dilution (Table 1.2). MICs measured using this method were significantly higher than what was required for growth inhibition via broth dilution. The concentrations listed in this table are the effective concentrations used to select for plasmids carrying various resistance cassettes utilized throughout this work.

Table 1.2. Antibiotic Minimum Inhibitory Concentration (MIC) on Agar Media

Strain	Kanamycin	Tetracycline	Gentamicin
P. protegens CHA0	50 μg/mL	60 μg/mL	50 μg/mL
P. protegens Pf-5	50 μg/mL	40 μg/mL	100 μg/mL
P. synxantha 2-79	>200 μg/mL	20 μg/mL	50 μg/mL
P. fluorescens Pf0-1	50 μg/mL	40 μg/mL	50 μg/mL
P. chlororaphis 30-84	50 μg/mL	40 μg/mL	100 μg/mL
P. ogarae F113	50 μg/mL	20 μg/mL	50 μg/mL
P. putida KT2440	100 μg/mL	100 μg/mL	100 μg/mL
P. fluorescens SBW25	100 μg/mL	60 μg/mL	50 μg/mL

Transforming DNA into Pseudomonas

In order to establish a genetics system in our *Pseudomonas* strains, methods of introducing exogenous DNA into these strains needed to be tested and quantified, if applicable. To do so, the pBBR1-MCS2 vector was used, which carries the broad host range pBBR1 origin of replication and has been reported to replicate in various *Pseudomonas* strains (31, 81, 82). Both electrotransformation and conjugation using donor strain *E. coli* WM3064 were attempted in the selection of Pseudomonads. Conjugation was an effective method of transferring plasmid DNA into all strains except *P. protegens* CHA0. Mating periods of 4, 8, and 16 hours were

attempted with *P. protegens* CHA0 on solid media. No transformants were isolated using this donor strain and conjugation for this *Pseudomonas* strain [data not shown].

In this work, electroporation variables are compared using two measurements: transformation efficiency (TE) and transformation frequency (TF). Transformation efficiency is a measure of number of transformants/µg DNA and is the standard way of reporting electroporation efficiencies. It assumes that transformation efficiencies change based on the amount of DNA available, which is true to an extent, although TE has an upward limit when a saturating amount of DNA is used. Reporting the overall efficiency of electrotransformation as solely TE ignores a very important variable: initial cell amount. To supplement this information, transformation frequencies are also included in most of the experiments performed in this section, which quantifies efficiency as a measure of number of transformants/survivor cells. For the most part, transformation efficiencies and transformation frequencies will follow similar trends, with some exceptions as observed later in this chapter.

Electroporation was the preferred method of introducing recombinogenic oligos into the cell for recombineering experiments, I performed my experiments utilizing log phase cells so replication forks would be present in the population, in accordance with the widely accepted mechanism of recombineering, discussed in Chapter 2. It should also be noted that I used unmethylated plasmid extracted from *E. coli* GM2163, as early transformation efficiencies seemed to be hindered by methylated plasmid (data not shown).

The effect of pulse voltage was first investigated in *P. protegens* CHA0 (Figure 1.4). Other variables of the pulse, 0.1 cm cuvette gap with, a capacitance of 25 µF, and resistance of 600 Ω were not manipulated. It was clearly evident that a pulse voltage of 1.2 kV resulted in highest transformation efficiencies for *P. protegens* CHA0. The transformation frequency was also highest when a pulse voltage of 1.2 kV was used. A pulse voltage of 2.5 kV when using log-phase cells was much too high and failed to produce any transformants. It should be noted that the survival rate was fairly consistent across all voltages tested, between 5×10^8 and 1.5×10^9 viable cells out of an estimated 2×10^9 cells present before harvesting. A pulse voltage of 1.2 kV was then used as the pulse voltage for all subsequent electrotransformations.

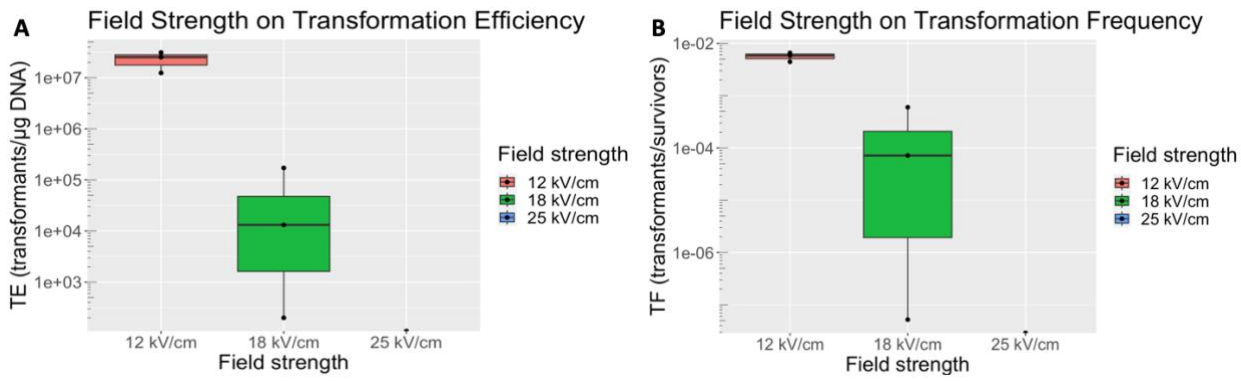

Figure 1.4. Comparison of field strength on electroporation. Three different pulse field strengths were compared in log phase cultures of *P. protegens* CHA0. Data are from single experiment with 3 biological replicates.

The effect of wash buffer was then investigated within a subset of the strains: *P. protegens* CHA0, *P. protegens* Pf-5, and *P. putida* KT2440 (Figure 1.5A). The four wash buffers tested were 1 M sorbitol (pH 7.6), 300 mM sucrose, 10% w/v glycerol, and water. The two buffers resulting in the highest transformation efficiencies, 1 M sorbitol (pH 7.6) and 300 mM sucrose, were tested in two additional strains, *P. fluorescens* Pf0-1 and *P. ogarae* F113. It was found that the most efficient buffer for *P. ogarae* F113 and *P. protegens* Pf-5 was 1 M sorbitol (pH 7.6), with a 10-fold increase in transformation efficiency observed in *P. ogarae* F113 when compared to 300 mM sucrose. *P. protegens* CHA0 transformed equally as well in 1 M sorbitol and 300 mM sucrose. Transformation efficiencies increased approximately 100-fold for *P. protegens* Pf-5 and *P. protegens* CHA0 in buffers 1 M sorbitol and 300 mM sucrose when compared to either 10% w/v glycerol or water. This 100-fold increase in transformation efficiency was not observed in *P. putida* KT2440 when comparing 1 M sorbitol and 300 mM sucrose to 10% glycerol or water, though there was a 10-fold increase when using 300 mM sucrose compared to 10% glycerol or water in this strain. The highest transformation efficiencies observed were in *P. protegens* CHA0 and *P. protegens* Pf-5 ($2 \times 10^7 - 7 \times 10^7$/µg DNA), followed by *P. ogarae* F113, and *P. putida* KT2440. Transformation efficiencies were approximately 1000-fold lower in *P. fluorescens* Pf0-1, estimated at 5×10^4-7×10^4/µg DNA when compared to the *P. protegens* strains.

Figure 1.5. Effect of wash buffer on *Pseudomonas* electrotransformation. Transformation efficiency **(A)** and transformation frequency **(B)** were compared using different wash buffers (1 M sorbitol (pH 7.6), 10% w/v glycerol, 300 mM sucrose, and water) in three *Pseudomonas* spp. Two additional strains were tested using the most effective wash buffers, 1 M sorbitol (pH 7.6) and 300 mM sucrose. All cells were harvested in log phase and electroporated using a pulse voltage of 1.2 kV. Data result from single experiments in biological triplicate.

Transformation frequencies when comparing different wash buffers predominantly followed the same trend, with the buffers resulting in the highest transformation efficiencies also resulting in the highest transformation frequencies (1.5B). The exception to this strain *P. ogarae* F113 when washed with 300 mM sucrose, which achieved a transformation frequency of ~1.0, indicating that each electroporation survivor received plasmid.

Electroporation was also successfully performed in *P. synxantha* 2-79, *P. fluorescens* SBW25, and *P. chlororaphis* 30-84 for routine plasmid transformation using the protocol described in section 1.5; however full experiments testing the effects of different buffers using

log phase cells for these strains have not been performed and accurate numbers of transformation efficiencies and frequencies under the established conditions cannot be provided at this time.

Table 1.3 Plasmid compatibility in *Pseudomonas.*

Plasmid	Origin of replication	Ability to replicate
pBBR1-MCS2	pBBR1	Yes
pACYC184	p15a	No
pUC119	pMB1	No
pJUMP24	pRO1600/ColE1	Yes
pJD866	RK2 derivative	Yes*

Presence of plasmid was further confirmed in each strain by PCR. *denotes a plasmid/oriC not tested in this study that is reported to replicate in *Pseudomonas.*

Determining compatible oriCs in Pseudomonas

Using either conjugation or electroporation, the ability of several plasmids to replicate in *Pseudomonas* was tested (Table 1.3). It was found that in addition to the pBBR1 oriC, the pRO1600 oriC also replicates in *Pseudomonas*, although the plasmid carried an addition ColE1 oriC for replication in *E. coli.* Other oriCs tested included p15a and pMB1. The RK2 oriC was reported to replicate in *P. putida* KT2440; however, that oriC was not tested in this study against these strains (84). Whether a plasmid was able to replicate or not was found to be uniform across all 8 strains investigated in this study. It was also found that the pBBR1 and pRO1600/ColE1 plasmids are compatible with each other in *Pseudomonas*, allowing for additional experimental flexibility in downstream applications.

Comparing Induction System P_{cym} in Pseudomona*s spp.*

In order to control expression of certain genes within a host, different genetic induction systems must be tested. For an induction system to be considered ideal, it would be tightly regulated, titratable, induce high gene expression, and utilize a low-cost substrate. Well-characterized inducible promoters include P_{lac}, P_{tac}, P_{Rha}, and P_{BAD} (85). In this work both the

P_{Cym} induction systems was tested using *gfp* expression plasmid pMR77 (86). The P_{Cym} system induces gene expression when the substrate molecule, cuminic acid (also known as cumate or p-isopropylbenzoate), binds to repressor protein CymR to open up the CuO operator sequence within the P_{Cym} promoter. It was originally isolated from *P. putida* F1 but has been adapted to work in several other model systems including *E.* coli, Gram-positive *Bacillus*, and DF1 and QM7 avian cells (87-89).

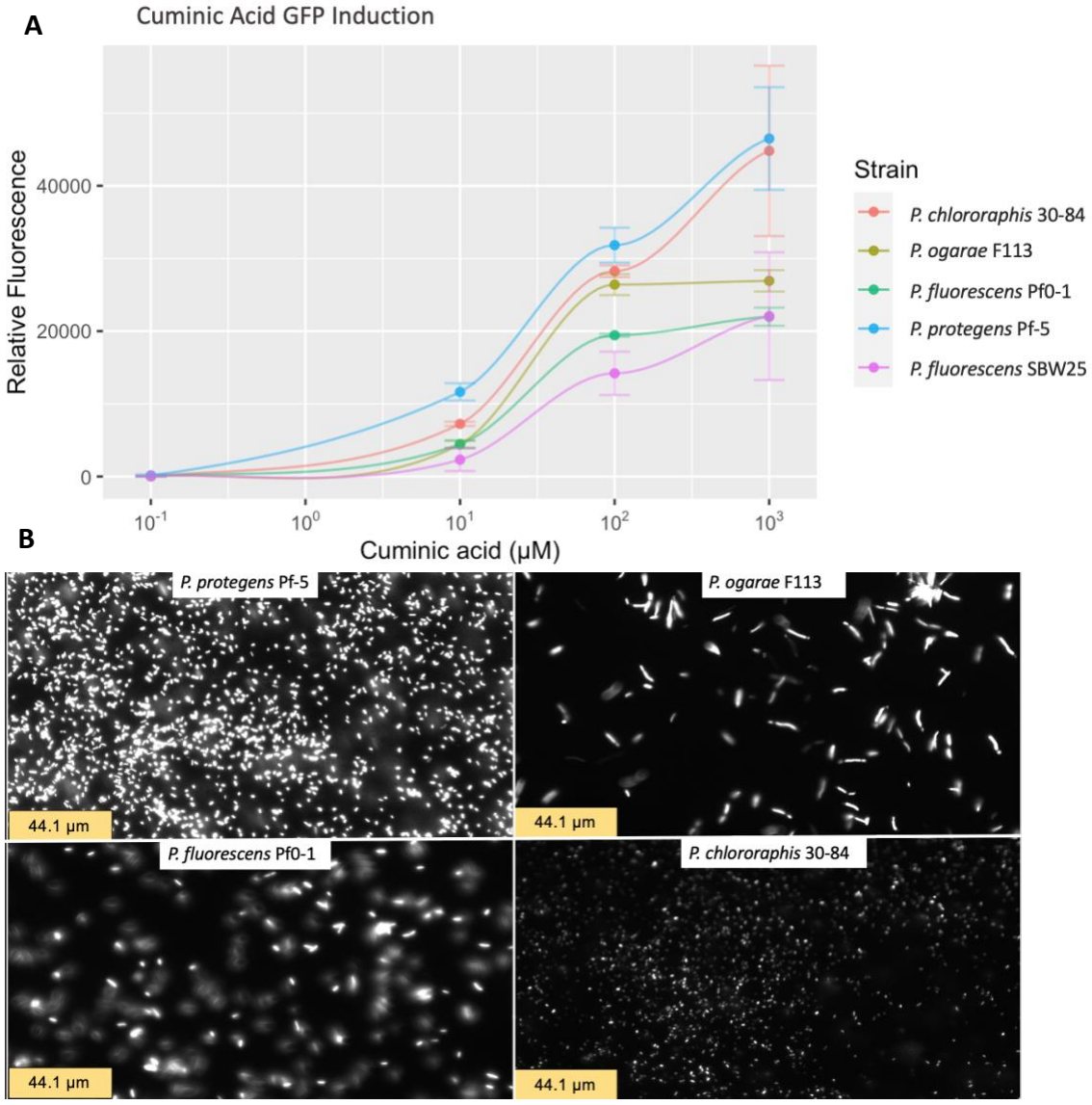

Figure 1.6. CymR-mediated induction of GFP in *Pseudomonas*. (A) *Pseudomonas* strains carrying the pMR77 inducible plasmid were induced overnight with increasing cuminic acid concentrations and relative fluorescence was reported. Data are representative of single experiment with two biological replicates. **(B)** Visualization of cuminic acid induced GFP expression using cells carrying plasmid pMR77 harvested after treated overnight with 1 mM cuminic acid.

The P_{cym} system was tested in a subset of the *Pseudomonas* strains across a range of inducer concentrations (Figure 1.6). It was found that variable fluorescence levels are obtained in the different strains, indicating that strength of induction by this system does likely vary some within the genus. The induction of GFP under the P_{cym} system was found to be dose-dependent based on concentration of inducer molecule, allowing for controlled expression of genes cloned under this system. Induction of GFP in strains *P. ogarae* F113 and *P. fluorescens* Pf0-1 appeared to saturate at a concentration of 100 μM cuminic acid, while all other strains tested resulted a ~1.5-fold increase in relative fluorescence when treated with 1 mM cuminic acid compared to 100 μM cuminic acid. Relative fluorescence increases from 10^{-1} to 10^{3} μM cuminic acid ranged from 426-fold in *P. fluorescens* Pf0-1 to 943-fold in *P. chlororaphis* 30-84. Fluorescence levels at 10^{3} μM cuminic acid in these strains was also visualized using fluorescence microscopy (Figure 1.6B).

1.6 Discussion

In this study, I aimed to lay out the rational initial steps in developing genetic systems in several strains of *Pseudomonas*, which I believe can largely be applied to colony forming Gammaproteobacteria. In the age of modern biology where new genomes are sequenced daily and gene editing tools are constantly evolving in both capability and method, it is easy to overlook the basics when presented with a new strain. Most modern gene editing tools including the clustered regularly spaced short palindromic repeat (CRISPR)-Cas9 system (90), multiplex-automated genome engineering (MAGE) (91), and long fragment editing (92), rest on the ability to introduce specific genes into a bacterium, modulate expression of those genes primarily via plasmid maintenance within a cell and promoter/RBS control, and select for bacteria with the desired genetic changes via selection or counterselection strategies. This generally requires knowledge of antibiotic MICs for plasmid selection, which plasmid origins of replication are compatible within a strain, and ways to introduce DNA into a cell.

Here I revisit these classical components of a genetics system in a selection of rhizobacterial *Pseudomonas* spp., which not only provides a general starting point to begin more developed studies within these strains but also highlights some of the strain-to-strain diversity within the *Pseudomonas* genus. As shown in this chapter, the differences between these strains

extend beyond G+C content, genome size, and reported plant growth-promoting properties, to varying lab treatment responses between strains.

I initially investigated the growth rates of these *Pseudomonas* strains on two different rich media: LB and King's B medium. Previous research indicated that both media are used to routinely culture these strains (33, 82, 93, 94). King's B medium is historically used as a differential medium to enhance production of pigments and fluorescent siderophores in *Pseudomonas*, as the media contains no added iron (95). A recent study by Shahid et al (2021) profiles the distribution of secondary metabolites and quorum-sensing molecules produced by a selection of *P. aurantiaca* and *P. chlororaphis* strains when grown in LB and King's B medium, highlighting the importance of media choice when considering future experiments (96). Generally, it was found that LB supports higher production levels of phenazines, while King's B medium enhanced pyrrolnitrin and siderophore pyochelin production, which I observed phenotypically in our *Pseudomonas* spp. (Appendix Figure 1.1). For our purposes, I wanted to determine if significant growth rate differences would be found and if one medium was generally preferred across the group. I found that LB supported faster growth rates in all strains, likely due to the availability of various carbon sources from yeast extract in LB compared to strictly glycerol in King's B medium, as well as the limitation of iron availability in King's B medium. The more pronounced growth defects in *P. chlororaphis* 30-84 and *P. synxantha* 2-79 when cultured in King's B medium compared to LB may be in response to the availability of carbon and iron. *P. chlororaphis* 30-84 has not been reported to produce siderophores, which may explain the slower growth phenotype in iron-limited King's B medium. While *P. synxantha* 2-79 does produce the siderophore pyoverdine, it has been reported to reach much lower biomass amounts when grown on glycerol as a carbon source compared to other sources like glucose, xylose, galactose, and mannose, which supports the slower-growth phenotype on King's B medium observed in this study (97).

Antibiotic profiling of a subset of the *Pseudomonas* strains highlighted the importance of performing in-house MIC determination for a newly acquired strain. In many cases, the MICs found in our investigation varied from those reported in other studies. This may be due to strain evolution over time while in the hands of different research labs as well as different MICs when grown on different media or with available lab materials (98-100). The distribution of susceptibility was fairly uniform across the subset of strains tested; however, interesting outliers

were identified via measured growth rates under different antibiotics treated. Specifically, *P. fluorescens* Pf0-1 was the only strain that had measurable growth inhibition when treated with ampicillin, although it has been reported to possess *ampC*, which encodes a β-lactamase, which typically causes resistance to β-lactam antibiotics (101). A BLAST search of the NCBI uploaded genomes for the subset of 6 strains tested against ampicillin with the *Pseudomonas aeruginosa* PAO1 *ampC* gene showed only *P. fluorescens* Pf0-1, *P. protegens* CHA0, and *P. protegens* Pf-5 carrying genes with significant alignments. Resistance to β-lactam antibiotics in *Pseudomonas* strains not carrying an *ampC* gene have been primarily credited to efflux pumps, which is likely the mechanism of resistance in the other strains tested (101). It is surprising that our collected strain of *P. fluorescens* Pf0-1 is susceptible to ampicillin given the encoded *ampC* present on the published genome (locus tag: PFL01_RS18695). It may be due to genome variability of the specific strain I inherited; sequencing of the *ampC* gene and surrounding gene neighborhood may indicate why our version is susceptible to ampicillin when I expect it to be resistant. The high resistance to kanamycin in *P. synxantha* 2-79 is another interesting characterization discovered in this work, as it is susceptible to the other aminoglycoside tested, gentamicin. Clinical isolates of *P. aeruginosa* found to be resistant to kanamycin but not to gentamicin were associated with kanamycin phosphotransferase activity (102). An initial BLAST search of a *P. aeruginosa* kanamycin phosphotransferase resulted in no significant similarities when compared to the *P. synxantha* 2-79 genome; however, an aminoglycoside 3'-phosphotransferase (locus tag C4K01_RS24140) was found on the *P. synxantha* 2-79 genome that is not present on the genomes of the other strains in this study, which may be the gene responsible for the kanamycin resistance observed in this strain.

The reported MICs for broth dilutions of these strains was much lower than what was required on solid media. This is a well-published phenomenon in *P. aeruginosa*, due to differences in magnesium and calcium concentrations in agar compared to broth (which I did not normalize for in this study) (99, 103, 104). Interestingly, the dependence on magnesium and calcium for antibiotic resistance has not been reported in the strains used in this study. Additional experiments both determining the baseline concentrations of cations available in agar compared to broth as well as testing multiple concentrations may help to establish a connection of MIC variability based on cationic titer. *Pseudomonas* is also widely known for increasing efflux pump activity under environmental stressors and as a mechanism for antibiotic resistance, so it was

expected that MICs on solid media would be higher than in liquid as the surface area in contact with the antibiotic when grown on solid media is much less (79, 105).

When establishing mechanisms of plasmid transfer into some of the *Pseudomonas* spp., another interesting characteristic was discovered. *P. protegens* CHA0 was not able to be conjugated using donor strain *E. coli* WM3064; however, it should be noted that conjugation was reported to work in *P. protegens* CHA0 using donor strain *E. coli* ET12567 (81, 106). The donor strain *E. coli* ET12567 is a methylation-negative strain, indicating that *P. protegens CHA0* may be especially sensitive to methylation patterns, which I observed canonically in our transformation attempts with methylated plasmid. The different strains showed variable tolerance to transformation with methylated plasmid (data not shown), possibly due to different restriction modification systems present in the strains. For example, a BLAST search for the type I restriction modification system *hsdM* reported in *P. protegens* Pf-5 (locus tag: PFL_2965) against the other strains in this study retrieved no significant similarity (25). These restriction modification systems exist to protect environmental strains from exogenous DNA and bacteriophage and likely all recognize different sequences, which may lead to differences in plasmid transfer based on plasmid sequence (107). Regardless, unmethylated plasmid isolated from *E. coli* GM2163 did not seem to have a deleterious effect on electrotransformation and is therefore recommended to increase efficiencies in wild strains.

Several electroporation variables were investigated in this study. The effect of voltage was so pronounced in *P. protegens* CHA0 that I assumed a voltage of 1.2 kV (the field strength equivalent of 2.5 kV for 0.2 cm cuvette) was appropriate for the other strains tested. This may not be the optimal voltage for all strains used in this study; however, it is the voltage that is reported across most references I came across involving electrotransformation in *Pseudomonas* (83, 108, 109). I also did not optimize electroporation based on cell volume or growth phase in this study; however, log-phase cells typically are optimal (110). These three variables could be further optimized for each strain and may help to improve electrotransformation in strains with lower efficiencies.

The choice of electroporation wash buffer was shown to have a strong effect on the efficiency and frequency of transformation across the 5 strains investigated, with up to 100-fold differences in efficiency and frequency within single strains reported based on choice of buffer. Electroporation wash buffers vary in conductivity and osmolality, which both affect the sample

resistance and cell survival (110). It is generally accepted that buffers with low conductivity are best for electroporation, and the osmolarity of the buffer is usually similar to that of the cell or slightly hypertonic. It is known that the conductivity of a solution is affected by its pH (Bio-Rad); however, I would expect the pH of these buffers to be somewhat similar and neutral, within the range of approximately 7 to 7.6. Measuring the conductivity of these various buffers may indicate why 300 mM sucrose and 1 M sorbitol (pH 7.6) consistently were the more efficient buffers, specifically in *P. protegens* CHA0 and *P. protegens* Pf-5. In this study I also tested a range of osmolality, from effectively 0 Osm in water to 1 Osm in 10% glycerol and 1 M sorbitol (pH 7.6). Buffer osmolality did not show a clear trend in influencing electroporation efficiency or frequency in this study, as the most effective buffers were 300 mM sucrose (300 mOsm) and 1 M sorbitol (pH 7.6)(1 Osm). Both of these buffers were hypertonic compared to normal cell osmolality (150-215 mOsm)(111). Regardless, the effect of wash buffer on transformation efficiency and frequency produces variable results across the five Pseudomonas strains; highlighting the importance of treating each strain uniquely and the difficulty to find a one-size fits all transformation protocol for a diverse genus.

The cuminic acid induction system was established to be compatible within the subset of strains tested. Variable levels of induction were achieved across the selection of strains, however, indicating that different concentrations of inducer may need to be used to normalize induction levels across the strains. Increased induction levels may be possible by optimizing RBS sequences for each strain, as well. The *cymR* system itself was confirmed to be a valuable induction method, as it allows for titratable control of induction over nearly 1000-fold ranges of expression. The cuminic acid molecule itself is relatively small, soluble, and can cross the cell membrane without the use of transporters. This allows relatively small amounts of inducer to be effective when compared to other induction systems (87). It appeared in our study that GFP expression in *P. ogarae* F113 and *P. fluorescens* Pf0-1 was saturated at 10^2 μM cuminic acid. Further experiments could help to establish the saturating concentration of inducer as well as the highest levels of GFP expression in the remaining strains.

1.7 Conclusion

The work highlighted in this chapter demonstrates many of the elements to be considered when working with a new strain. Though the *Pseudomonas* genus is fairly well-studied, strain to

strain diversity creates obstacles when implementing a genetics system, and nearly each strain studied in this section has shown some sort of unique behavior: *P. protegens* CHA0 cannot be conjugated using the same *E. coli* donor strain that is sufficient for all others, *P. synxantha* 2-79 is extremely kanamycin resistant, *P. ogarae* F113 is the only strain susceptible to ampicillin and has a very high transformation frequency using 300 mM sucrose, *P. putida* KT2440 is the only strain to prefer 300 mM sucrose as an electroporation buffer.

A main limiting factor preventing a more robust survey of these strains was time. Future work to expand upon the experiments performed in these strains from subsets to all 8 would provide a more complete picture of the variable behavior observed in these strains under different treatments. However, I conclude that even with a study emphasis placed on 4-6 of these strains, it is easy to see how each is unique in the context of a research lab. Using the results established in this chapter opens up the availability to do more complex experimentation in these strains in the future.

1.8 Materials and Methods

Bacterial Strains

All strains and plasmids used in this work are listed in Table 1.4. *P. protegens* Pf-5, *P. protegens* CHA0, *P. fluorescens* Pf0-1, *P. ogarae* F113, *P. chlororaphis* 30-84, *P. synxantha* 2-79, *P. putida* KT2440 and *P. fluorescens* SBW25 were obtained from Lawrence Livermore National Laboratory (Livermore, CA). LB medium (BD Difco™ Dehydrated Culture Media: LB Broth, Miller) was used to routinely culture bacteria. Solid media was supplemented with 1.5% w/v agar (Fisher BioReagents™ Agar, Powder / Flakes). Growth media was supplemented with kanamycin at a final concentration of 50 µg/mL for *P. protegens* Pf-5, *P. protegens* CHA0, *P. fluorescens* Pf0-1, *P. ogarae* F113, *P. chlororaphis* 30-84, and the routine *E. coli* strains used for cloning and conjugation, while a concentration of 100 µg/mL was used for *P. putida* KT2440 and *P. fluorescens* SBW25. Cultures were grown aerobically at 30˚C (*Pseudomonas sp.*) or 37˚C (*E. coli*) and shaken at 250 rpm.

Table 1.4. Strains and plasmids used in this work

Strain or plasmid	Description	Reference or source
UQ950	*E. coli* DH5α λ (pir) host for cloning	(Saltikov & Newman 2003)
GM2163	*E. coli* dam^-, dcm^-, CmR	CGSC#: 6581
JG3849	*E. coli* MG1655, F^- λ^- $ilvG^-$ rfb-50 *rph-1*	Gralnick Lab
JG49	*E. coli* UQ950, pBBR1-MCS2	Gralnick Lab
JG186	*E. coli* WM3064, Δ*dap* mating strain	Gralnick Lab
JG166	*E. coli* WM3064, pBBR1-MCS2	Gralnick Lab
JG3470	*E. coli* WM3064, pUC119	Gralnick Lab
JG3472	*E. coli* WM3064, pACYC184-RP4	Gralnick Lab
JG4366	*P. protegens* CHA0	LLNL
JG4367	*P. protegens* Pf-5	LLNL
JG4368	*P. synxantha* 2-79	LLNL
JG4369	*P. fluorescens* Pf-01	LLNL
JG4370	*P. chlororaphis* 30-84	LLNL
JG4371	*P. ogarae* F113	LLNL
JG4405	*P. fluorescens* SBW25	LLNL
JG4406	*P. putida* KT2440	LLNL
JG4423	*E. coli* HST08, pMR77	LLNL
Plasmid		
pBBR1-MCS2	pBBR1 ori, Km^R	
pUC119	pMB1 (pUC) ori, Tet^R	Gralnick Lab
pACYC184-RP4	p15a ori, Tet^R	Gralnick Lab
pMR77	pRO1600 ori, pMB1 (pUC) ori, $Gent^R$, P^{Cym}, gfp	84

Growth rate comparison in different rich media

Comparison of growth rate in LB (BD Difco™ Dehydrated Culture Media: LB Broth, Miller: 10 g/L tryptone, 5 g/L yeast extract, 10 g/L NaCl) and King's B Medium (HiMedia™ : King's medium B base: 20 g/L proteose peptone, 1.5 g/L dipotassium hydrogen phosphate, 1.5 g/L magnesium sulfate heptahydrate, 15 mL/L glycerol) was performed. Frozen stocks of each strain were struck onto LB plates, and single colonies were then inoculated into LB or King's B culture in biological replicates and grown overnight at 30˚C and 200 rpm. Cultures were diluted 1:100 into 2 mLs of respective culture to a starting OD_{600} of ~0.02, and grown in the same conditions as above. The OD_{600} was measured at various timepoints over a 24-hour period. Respective doubling times in each media (Appendix Table 1.1) were calculated by estimating the slope of the exponential phase of each growth curve and the equation doubling time = log(2)/m.

Antibiotic minimum inhibitory concentration (MIC) assays

Determination of MICs in the different *Pseudomonas* strains was initially performed in liquid culture. Single colonies from freshly streaked frozen stocks were inoculated into LB culture and grown overnight. Cells were then inoculated into 100 µL of LB with respective antibiotic at a starting concentration of 0.01 OD_{600} in a 96-well plate wrapped with Parafilm and were statically incubated at 30˚C. The OD_{600} was quantified to measure cell growth at 0, 18, and 24 hours and was compared to an LB-only positive control. MICs on solid media were determined by plating an OD_{600}-estimated 10^9 cells onto LB agar plates containing various antibiotic concentrations. The MIC was determined as the concentration at which no colonies grew. Concentrations tested were as follows (in µg/mL): kanamycin, 25, 50, 100, 200; gentamicin, 25, 50, 100, 200; tetracycline, 10, 20, 40, 60, 100. Presence/absence of antibiotic resistance genes were determined using BLASTN under standard parameters using the following queries: *ampC,* NC_002516.2:4594029-4595222 *Pseudomonas aeruginosa* PAO1, complete genome; kanamycin phosphotransferase, NC_009656.1:c3858355-3857561 *Pseudomonas aeruginosa* PA7, complete sequence; aminoglycoside 3'-phosphotransferase, NZ_CP027756.1:5214724-5215494 *Pseudomonas synxantha* strain R6-28-08 chromosome, complete genome.

Plasmid transformation

To initially determine plasmid compatibility in each *Pseudomonas* strain, both conjugation and electroporation were attempted. Conjugation was performed by cross-streaking a colony of mating strain *E. coli* WM3064 carrying the intended plasmid for transformation with a colony of wildtype *Pseudomonas* on an LB plate with 250 µM 2,6-diaminopimelic acid (DAP). After a mating period of 4 hours-overnight, the mating biomass was resuspended in 100 µL of LB and plated on LB supplemented with the appropriate antibiotic for selection in each *Pseudomonas* strain.

Electroporation optimization

Single colonies were inoculated into 3 mLs of LB and grown overnight at 30˚C and 250 rpm. Cultures were diluted to an OD_{600} ~ 0.085 and grown in the same conditions until they reached an OD of 0.4-0.6, as downstream applications would require log phase cells. 4 mLs of culture were used per replicate. Cells were harvested by centrifugation at 10,000 rpm for 1 minute. Cell pellets were gently washed three times by resuspension in 1 mL of indicated wash buffer when comparing wash buffers: 1 mL of 1 M sorbitol (pH 7.6), 300 mM sucrose, sterile MilliQ water, or 10% glycerol; or by 1 M sorbitol (pH 7.6) when comparing pulse voltages. Each wash was followed by centrifugation under the same conditions as above, decanting the supernatant each time. After the final wash, cells were resuspended in a final volume of 60-70 µL and 250 ng of $dam^{-}dcm^{-}$ pBBR1-MCS2 was mixed into the cell suspension. The cell suspension was transferred into a 0.1 cm cuvette (Bio-Rad: Gene Pulser Cuvette, E. coli Pulser Cuvette) and a pulse was applied (settings: 25 µF; 200 Ω; 1.2 kV (unless otherwise specified) on a Bio-Rad GenePulserXcell™; Bio-Rad). 1 mL of LB was added, and cells were transferred to a 2 mL Eppendorf tube to recover at 30˚C and 250 rpm for 2 hours. 1:10x cell dilutions were plated on LB and LB with kanamycin to quantify number of viable cells and transformants.

Transformation efficiency was calculated by dividing number of transformants by amount of plasmid (ng), and transformation frequency was calculated by dividing number of transformants by number of viable cells. M13 primers were used to confirm plasmid transformation with pBBR1-MCS2.

For routine plasmid transformation, 1 M sorbitol (pH 7.6) and a pulse voltage of 1.2 kV was used. 50-250 ng of plasmid DNA was sufficient to generate transformants.

Presence/absence of type I restriction modification system was performed using BLASTN under standard parameters using the query NC_004129.6:c3324929-3323187 Pseudomonas protegens Pf-5, complete sequence.

Comparing Induction System P_{cym} in Pseudomonas spp.

To compare induction of Gfp by the *cymR* system in different *Pseudomonas* sp., strains carrying the pMR77 plasmid were freshly struck from frozen stocks. Single colonies were inoculated into LB + kanamycin and various cuminic acid concentrations for overnight growth and induction. A normalized volume to an OD_{600} of 2 was harvested, washed twice with PBS (NaCl, 8 g/L; KCl, 0.2 g/L, Na_2HPO_4; 1.44 g/L; KH_2PO_4, 0.245 g/L), resuspended to a final volume of 100 µL, and transferred to a black 96-well plate (get info). Relative fluorescence was measured using a microplate reader (Agilent BioTek Synergy LX Multimode Reader, Santa Clara, CA) using the settings of excitation at 485/20 nm, emission at 540/20 nm, and a gain of 35.

Chapter 2: Development of recombineering system in *Pseudomonas* spp.

2.1 Aim of this work

In this chapter, I aim to utilize the components of a genetics system investigated in Chapter 1 to establish a recombineering system in a subset of *Pseudomonas* strains. Here I choose to restrain our study to strains with the highest measured transformation efficiencies, *P. protegens* Pf-5, *P. protegens* CHA0, and *P. putida* KT2440, as a key step in our recombineering scheme involves introducing recombinogenic oligonucleotides by electroporation. Attempts with other strains *P. fluorescens* Pf0-1 and *P. ogarae* F113 have not provided positive recombineering results thus far, which I attribute to the limitation of transformation efficiency observed in these strains (as seen in Chapter 1). I also investigate the effect of oligonucleotide protection via phage protein Gam as well as chemical modification by phosphothiolation treatment specifically in *P. protegens* Pf-5.

2.2 Abstract

While the development of robust genetic tools has been prioritized extensively in *E. coli*, the application of these frameworks to other bacteria are often less successful. The adaptation and optimization of wild bacteria for anthropogenic use is inherently valuable for industrial and agricultural applications. One group of bacteria with high potential to this end are the plant-growth-promoting rhizobacteria (PGPR) in the *Pseudomonas* genus. In this work I investigate the use of four phage-encoded recombinases to develop a recombineering workflow in 3 PGPR strains: *P. protegens* Pf-5, *P. protegens* CHA0, and *P. putida* KT2440. Using Rif^R point mutations in the *rpoB* gene, I reach maximum recombineering efficiencies of 1×10^{-4}, 5×10^{-4}, and 2×10^{-5}, respectfully, in these strains using λ-Red Beta recombinase from *E. coli* BL21DE3. I further examine recombineering efficiencies in *P. protegens* Pf-5 as a function of DNA substrate load amount, phosphorothiolate bond protection, and Gam protein coexpression. These results support the potential of recombineering as a useful platform to generate mutations in *Pseudomonas,* as well as identify future adaptations to improve this system.

2.3 Overview of Recombineering

Recombineering, or recombination-mediated genetic engineering, is a gene editing method which utilizes prophage-derived proteins to introduce precise mutations into a dividing cell (112, 113). These recombination proteins integrate linear DNA substrates into the host chromosome or plasmid during replication, requiring only 40-50 nucleotides of oligonucleotide homology to the genetic target (113-115). Two major families of prophage recombination proteins are utilized in most recombineering schemes today: the λ-Red phage and the Rac phage from *E. coli*, though homologous proteins found in phage regions of other bacteria have also been shown to be effective recombinases for recombineering schemes (116-118). The λ-Red phage suite of recombination proteins includes three proteins: Beta, Exo, and Gam—while the Rac prophage recombination proteins consist of RecT and RecE (119). The Beta and RecT proteins are single stranded DNA annealing proteins (SSAPs) that bind to single stranded DNA and facilitates annealing to homologous DNA as an Okazaki fragment (119). SSAPs are characterized by the formation of an oligomeric ring around the ssDNA as well as performing annealing of the DNA fragment in an ATP-independent fashion (120). Exo or RecE are 5' to 3' exonucleases which degrade double-stranded DNA (dsDNA) into a ssDNA substrate for Beta or RecT annealing (113, 119). The Gam protein is an inhibitor of the RecBCD and SbcCD enzymes, a family of exonucleases, endonucleases, and helicases that degrade foreign dsDNA and ssDNA as part of host restriction modification systems (119). Expression of Gam in recombineering systems can be used to protect recombinogenic oligonucleotides from degradation (119, 121).

Recombineering revolutionized the field of genetics as it allowed scarless mutations to be introduced into either plasmids or the bacterial chromosome at a relatively low cost compared to earlier methods. RecA-driven recombination, which had been the gold standard in the field for decades, required the introduction of large pieces of DNA, typically on suicide plasmids, which requires multiple steps of cloning and selection to generate the desired mutant (112, 122). RecA is a protein involved in DNA repair that relies on long regions of homology (500-2000 bp) to repair dsDNA breaks or introduce mutations via strand invasion (112). It's found in nearly all bacteria, and therefore was the primary method to manipulate a host's genome (123, 124). Recombineering, however, is far faster and cheaper as oligonucleotides can be easily customized

and synthesized for different locations based on the relatively short regions of homology required for phage-derived recombinases.

Initial ssDNA recombineering efficiencies in lab strain *E. coli* HME5 using λ-Beta for single-nucleotide polymorphisms were ≈ 0.2 % recombinants per viable cell (115). Method optimization has increased this value to ~30% in *E. coli* (125). The main adaptations to improve recombineering efficiencies centered on oligonucleotide design, including optimizing homology arm length, minimizing oligo hairpins or other secondary structures, using oligos with low off-target binding homologies, and targeting oligos to bind to the lagging strand of the replication fork (113, 125); however, strain engineering by deleting mismatch repair protein MutS was another instrumental change in improving recombineering efficiency, although this change can create genome instability and increase off-target mutations (84)(125)(126). Further strain innovation to remove exonucleases including ExoI and RecJ have also improved recombineering efficiencies (127). Attempts at recombineering in other genera including *Lactobacillus, Corynebacterium, Pseudomonas* and even wild *E. coli* strains have not yet reached these high levels of efficiency (84, 128-131). These high levels of recombineering efficiencies generated in laboratory *E. coli* strains are attractive to geneticists as they expand the capability of genome editing to include more intensive changes employed by the Multiplex Automatable Genome Engineering (MAGE) platform, which allows the introduction of multiple mutations synonymously to generate large mutant pools over several cycles with relatively low cost, time, and effort (91, 132). Difficulties with applying this platform in other genera have been attributed in part to using hosts with less understanding and prior genome modifications than laboratory strains of *E. coli* as well as recombinase portability issues (117, 133).

Recent reports have highlighted interesting interactions between different host systems and preference for recombinase. While it is generally accepted that application of recombination proteins is partially dependent on phylogenetic distance, it was recently shown that this host-dependent tropism may be due to interactions between the chosen recombineering-encoded proteins and host machinery. Filsinger, et al. (2020) discovered a key interaction that affects the portability of recombineering schemes by identifying a C terminal 7-amino acid sequence within host single-stranded DNA-binding proteins (SSB) that determine whether a specific RecT family (including λ-Beta) recombinase is compatible or not. With compatible SSBs, the recombineering efficiencies improved up to 1,168-fold in a previously recalcitrant species, *Lactobacillus lactis*

(116). This is possibly due to the inability of a specific recombinase to displace host SSBs to facilitate oligo strand annealing (112, 114, 134, 135).

The high levels of recombineering efficiency in *E. coli* allows for the identification of positive clones without the need for positive selection or counterselection strategies. To work around the limitation of low recombineering frequencies, early recombineering frameworks involved the inclusion of a positive selection marker, like an antibiotic cassette, flanked by Cre or FLP recombinase sites to remove the drug marker in a second step on the sequence of the recombinogenic oligonucleotide (112). This selection method left behind *loxP* or *frt* recognition sites, thus creating a scar next to the desired mutation. The *sacB* gene has also been utilized in recombineering as a counterselection method to remove a drug marker from an integrated recombinogenic mutation (128). The *sacB* gene encodes levansucrase, which produces a toxic product inducing cell death when sucrose is present (136), which enables scarless mutations to be made for a non-selective mutation. Mutations in the *sacB* gene, however, occur at a rate of approximately 0.01%, so false positive recombinants may occur in the population and would require additional screening for positive clones (112). Over the last few years, the site-specific Cas9 endonuclease from *Streptococcus pyogenes* has been coupled to recombineering to create a powerful counterselection tool against non-edited bacteria within a population (84, 90, 119, 131, 137). The Cas9 endonuclease cleaves dsDNA at a specific nucleotide sequence encoded by a guide RNA molecule, which allows targeted selection against bacteria that have not successfully introduced the desired mutation into the genome (138). Cas9 counterselection removes the requirement of introducing a selectable mutation, effectively opening up the genome to introduce mutations at nearly any site with high apparent efficiencies of >90% in most cases (84, 131, 139). This method of counterselection does come with its own set of limitations as the number of mutations that can be introduced and selected for is generally restrained to a 2-3 encoded by specific guide RNA sequences (139, 140). Cas9 counterselection also requires the desired mutation site to be within 20 nucleotides of an NGG PAM site for Cas9-directed cleavage (138).

2.4 Summary of efforts to date in *Pseudomonas*

Previous research in implementing a recombineering platform in *Pseudomonas spp.* has primarily focused on a few strains and a few recombinases (Table 2.1). Lesic and colleagues were the first to attempt recombineering in *P. aeruginosa* PA14 in 2008 using the λ Red suite of

proteins, with actual efficiencies on the order of 10^{-9} reported, even using long homology arms from 400-600 nt (141). These efficiencies were improved by the discovery of RecTE homologs in the *P. syringae pv. syringae* B728a strain, which has to date been tested in a few *Pseudomonas* strains (108, 142). In this study I will expand upon current data of this recombinase, as well as testing additional recombinases in environmentally relevant strains *P. protegens* Pf-5, *P. protegens* CHA0, and *P. putida* KT2440.

Table 2.1. Overview of Select Recombineering Efforts to date in *Pseudomonas spp.*

Strain	System reported with highest efficiency	Substrate	DNA Load† (approx.)	Genetic Target	Efficiency*	Reference
P. aeruginosa PA14	pUCP-RedS (Arabinose-induced λ Red Beta, Exo, Gam)	PCR product with 100 bp homology arms	7×10^{12} copies	Δ*pqsC*::kan (800 bp insertion)	3.4×10^{-9}	Lesic, 2008
P. syringae pv. tomato DC3000	Constitutively expressed RecT/E from *P. syringae* pv. syringae B728a	ssDNA with 40 bp homology arms	1.2×10^{14} copies	4 bp mutation K43R in *rpsL*	2.4×10^{-4}	Swingle, 2010
		PCR product with 91 bp homology arms	5×10^{12} copies		4.5×10^{-9}	Swingle, 2010
P. putida KT2440	M-toluic acid inducible λ Red Beta, Exo, Gam	PCR product with 500 bp homology	5.4×10^{11} copies	Δpp_0589::kan (800 bp insertion)	2.7×10^{-7}	Luo, 2016
	M-toluic acid inducible RecT/E from *E. coli* MG1655	PCR product with 100 bp homology	2.6×10^{12} copies	Δpvd::tetA (1.1 kB insertion)	5×10^{-8}	Choi, 2018
	M-toluic acid inducible λ Red Beta	ssDNA with 50 bp homology	1.2×10^{14} copies	1 bp mutation (kan knock-in)	2×10^{-3}	Wu, 2019
P. putida KT2440	Constitutively expressed λ Red Beta	ssDNA with 45 bp homology	3×10^{14} copies	4 bp Q518L change in *rpoB*	2×10^{-5}	This study

P. putida EM42 (KT2440 derivative)	3MB inducible Ssr T1E_1405 from *P. putida* DOT-T1E	ssDNA with 45-50 bp homology	2.9 x 10^{13} copies	100 bp deletion in *pyrF*	5 x 10^{-4}	Aparicio, 2016
P. protegens Pf-5	Rhamnose inducible RecT/E from *P. syringae* pv. syringae B728a and λ Red Gam	PCR product with 100 bp homology	1 x 10^{13}	Gentamicin cassette onto plasmid	1.5 x 10^{-6}	Yin, 2019
	Constitutively expressed λ Red Beta	ssDNA with 45 bp homology	3 x 10^{14} copies	15 bp D521P change in *rpoB*	1 x 10^{-4}	This study
P. protegens CHA0	Constitutively expressed λ Red Beta	ssDNA with 45 bp homology	3 x 10^{14} copies	15 bp D521P change in *rpoB*	5 x 10^{-4}	This study

*Efficiency selected from highest reported in single study or calculated based upon data provided.

† Calculated based on reported DNA substrate length and amount using following equation

$$Number\ of\ copies = \frac{Amount\ (ng) \times 6.022\ \times 10^{23}}{Length\ (bp)\ \times 1 \times 10^{9}\ \times Mass\ of\ DNA\ bp}$$, where mass of DNA bp is estimated as 660 for dsDNA, and 330 for ssDNA when sequence is not provided.

2.5 Choosing a genetic target

One of the challenges in a recombineering scheme is determining a target. I began initial recombineering attempts with *Pseudomonas lacZ*$^{\pm}$ strains, where the *lacZ* gene was inserted at a neutral site downstream of *glmS*, and a recombinogenic oligonucleotide that introduces both a frameshift and stop codon simultaneously. Successful clones would then be phenotypically white when plated on medium containing 5-bromo-4-chloro-3-indolyl-β-D-galactopyranoside (X-gal), while wildtype cells would remain blue, allowing for "blue-white" a visually screenable recombineering phenotype. This target, however, proved unsuccessful as recombineering frequencies would realistically have to be above 1 x 10^{-3} at minimum to potentially find the correct clone. As I were unable to find a single recombineered colony after several attempts [data not shown], I decided to test another target. Based on previous research (Table 2.1), recombineering efficiencies to date in *Pseudomonas* all required a selectable mutation, as it is nearly impossible to find a correct clone at these lower efficiencies. Initial recombineering

schemes in the field utilized the integration of antibiotic cassettes to find successful recombinants; however, recombineering efficiencies of integrating larger genes are much lower than smaller insertions or point mutations (Table 2.1)(119, 130). Several positive selection targets requiring smaller mutations have been explored in both *E. coli* and *Pseudomonas* spp., including *rpsL, pyrF, tolC, gyrA,* and *rpoB* (108, 117, 130). In each of these targets, either selective point mutations or insertion of premature stop codons can result in a genotype that can be selected for on specific media. To that end, I decided to investigate the use of mutating *rpoB* as a selectable recombineering target.

The *rpoB* gene encodes the Beta subunit of RNA polymerase, a gene essential to growth as it enables transcription. The antibiotic rifampicin binds to the RNA elongating pocket of RpoB, ultimately resulting in cell death. Specific point mutations in the *rpoB* gene can prevent this binding while retaining transcriptional activity, resulting in rifampicin resistant (Rif^R) bacteria. Additionally, the *rpoB* gene has been used extensively to estimate mutation frequency rate in bacteria, which provides further insight on the rate of random Rif^R clones compared to that resultant of recombineering (143). A majority of Rif^R mutations are concentrated within the rifampicin binding pocket, which are notated Clusters I and II (Figure 2.1). To that end, I performed analysis on spontaneous Rif^R mutants in five *Pseudomonas* strains by sequencing Clusters I and II of the *rpoB* gene after selection on rifampicin, as the identity of Rif^R mutations has been shown to be different across *P. aeruginosa* and *P. putida* KT2440 strains (144).

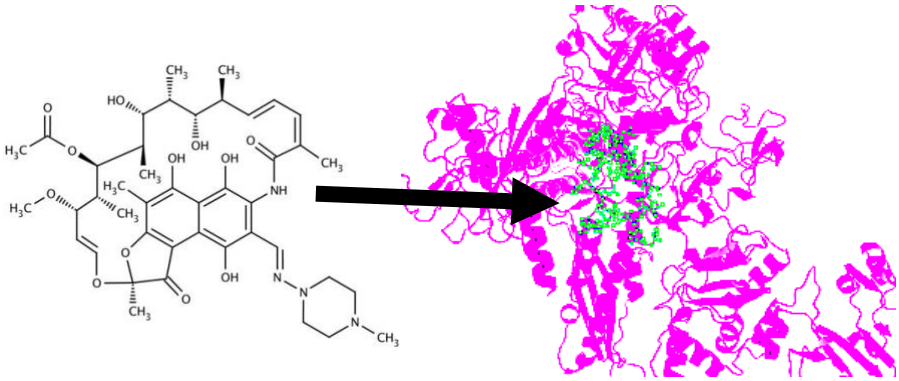

Figure 2.1. Rifampicin binding to RNA pol B. Structure of rifampicin molecule and its binding location within RNA polymerase B which blocks initiation of transcription. The binding location (Clusters I and II) residues are highlighted green. RNA polymerase B was modeled using Pymol.

2.6 Results

Table 2.2. Rifampicin resistant mutation rates in *Pseudomonas*.

Strain	Rif^R mutation rate
P. putida KT2440	1.5×10^{-7}
P. protegens Pf-5	2×10^{-8}
P. protegens CHA0	2×10^{-8}
P. fluorescens Pf0-1	2.8×10^{-8}
P. ogarae F113	3.3×10^{-8}

Identification of possible rpoB *recombineering mutations*

In order to find rifampicin resistance encoded point mutations within our selection of *Pseudomonas* spp., I first plated an overnight culture of 10^9 cells onto LB agar with rifampicin at concentrations of 25 µg/mL, 50 µg/mL, or 100 µg/mL. I saw higher levels of resistance at concentrations of 25 µg/mL, while rates of Rif^R were comparable at 50 µg/mL and 100 µg/mL. The Rif^R mutation frequencies for overnight cultures at a rifampicin concentration of 50 µg/mL are listed in Table 2.2. Differences in colony sizes were observed, likely indicating varying strengths of rifampicin binding inhibition caused by different mutations. After 24 hours of growth, I then sequenced Rif^R 10 colonies for each strain over Clusters I (amino acid 510-542) and II (amino acids 562-575) of the *rpoB* gene (Table 2.3). All of the mutations identified in this study were located in Cluster I, specifically between amino acids 517 and 536. A mutation hotspot occurs at amino acid residue 521 for all of the *Pseudomonas* strains tested, with the most common being an A → G transition mutation resulting in the exchange of glycine for aspartic acid. As this seemed a robust Rif^R mutation across all strains, I designed a recombinogenic oligo for this target in *P. putida* KT2440. Jatsenko et al. also reported the Q518L point mutation being prevalent in *P. putida* KT2440, so I designed a second recombinogenic oligo for that target as well (144).

Table 2.3. Rif^R mutations in *Pseudomonas*

Strain	Position	Nt change	Mutation	# mutants
P. fluorescens Pf0-1	1549	C → T	S517L	2
P. ogarae F113	1553	A → G	Q518R	1
P. protegens Pf5	1561	G → A	D521N	1
P. protegens CHA0	1562	A → G	D521G	1
P. ogarae F113	1562	A → G	D521G	2
P. fluorescens Pf0-1	1562	A → G	D521G	2
P. protegens Pf5	1562	A → G	D521G	7
P. putida KT2440	1562	A → G	D521G	10
P. fluorescens Pf0-1	1562	A → C	D521A	6
P. protegens CHA0	1567	A → G	N524D	1
P. protegens CHA0	1580	C → T	S527F	1
P. ogarae F113	1580	C → A	S527Y	1
P. ogarae F113	1592	A → T	N531L	1
P. ogarae F113	1592	A → G	N531R	1
P. protegens CHA0	1599	C → T	Silent	1
P. ogarae F113	1607	C → T	S536F	1
P. protegens CHA0	1650	C → T	Silent	1
P. protegens Pf5	1706	C → T	P569L	1
P. protegens Pf5	1736	C → T	S579F	1

Recombineering of rpoB in Pseudomonas

I tested the ability of 4 different recombinases to introduce two different Rif^R mutations in three *Pseudomonas* strains: *P. putida* KT2440, *P. protegens* Pf-5, and *P. protegens* CHA0. An overview of the recombineering approach used in this study is in Figure 2.2. Briefly, recombinogenic oligos were introduced via electroporation into log-phase cultures of each strain carrying plasmid pMK3a-d, which constitutively express RecT from *P. syringae pv. syringae* B728a, RecT from *E. coli* MG1655, λ Red-like W3 Beta from *Shewanella sp.* W3-18-1, or λ Red Beta from *E. coli* BL21DE3. Three Rif^R oligos encoded the Q518L, D521G, or D521P mutation with flanking silent mutations to create a mismatch length of either 4bp or 16 bp to evade MMR. After a 3.5-hour recovery period, cultures were plated on rifampicin containing media, and Rif^R

colonies were quantified after 48-96 hours. Presence of recombinase-dependent mutation was confirmed by colony PCR and Sanger sequencing, but not robustly quantified (Appendix Figures 2.1 and 2.3).

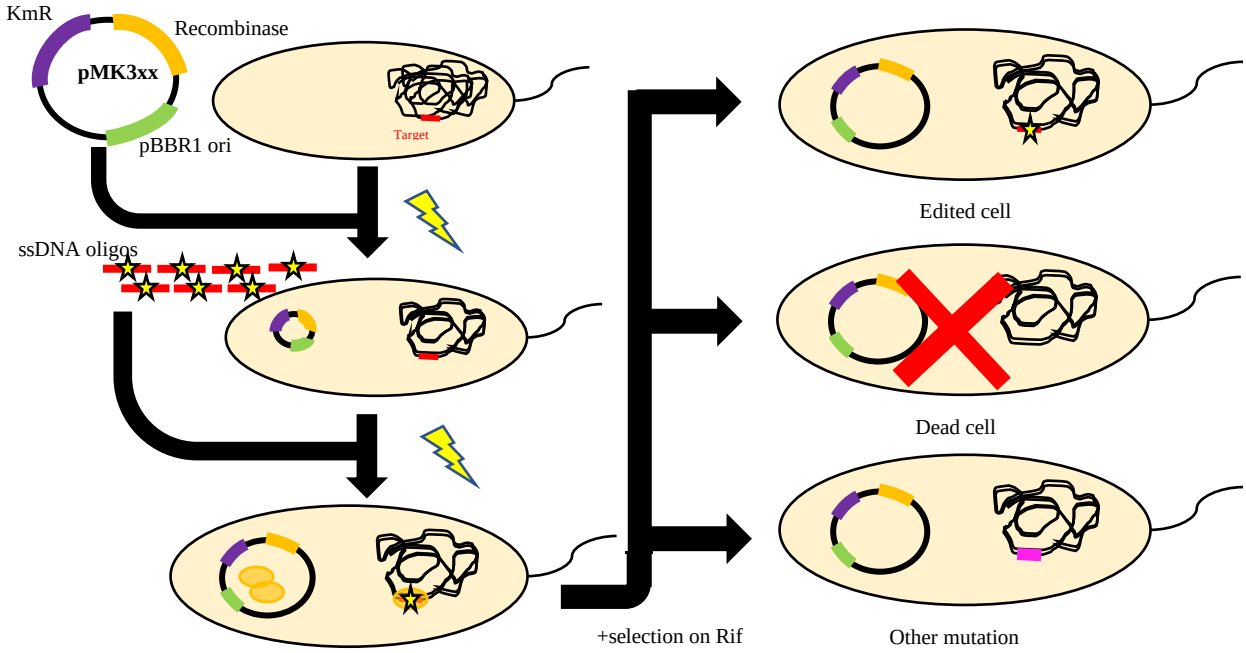

Figure 2.2. Overview of recombineering methodology. The selected recombinase is first electroporated into a chosen strain via electroporation of pMK3x plasmid. Strains harboring a pMK3x recombinase plasmid are grown to log phase and harvested for a second round of electroporation in which ssDNA Rif^R oligos are introduced. Cultures are then plated on rifampicin-containing media and LB after a recovery period, and Rif^R mutants and total viable cells are quantified after 48 hours of growth. Each cell has three possible outcomes: recombineered Rif^R, another Rif^R mutation, or death.

Based on previously reported recombineering attempts in *P. putida* KT2440, I chose the *P. syringae* RecT and *E. coli* λ Red Beta recombinases to test in this strain (Figure 2.3). Recombineering attempts in *P. putida* KT2440 with the maximum frequency of Rif^R mutants reaching ~2 x 10^{-5} using *E. coli* λ Red Beta. I were also only able to see clear differences in Rif^R frequencies when using the Q518L oligo. This was surprising, as the D521G mutation was present in all 10 Rif^R colonies sequenced in our prior *rpoB* mutation studies. The frequency of Rif^R colonies with oligo added was the highest in wildtype *P. putida* KT2440, which could indicate these recombinases tested may actually impair oligo recombination. More likely, the data presented here require additional experiments to improve recombineering efficiencies, as the increased frequency of Rif^R mutants in wildtype *P. putida* KT2440 may be an artifact of comparing efficiencies on relatively small scale with limited replicates.

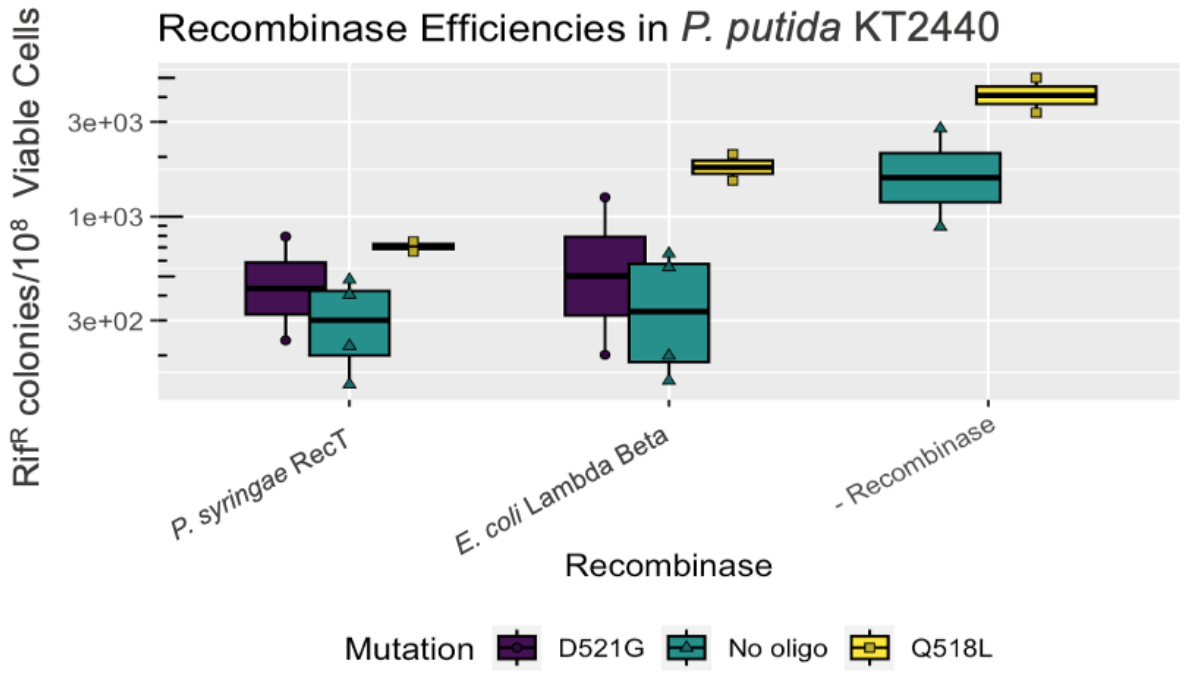

Figure 2.3. Recombineering of *rpoB* using *P. putida* KT2440. The effect of 2 different recombinases was examined in *P. putida* KT2440 using the D521G point mutation (16-bp mutagenic region) or the Q518L mutation (4-bp mutagenic section). The D521G oligo was not tested in strains without recombinase. 15 µg of oligo was electroporated into log phase cells, and the cell mixture recovered for 3.5 hours in LB before plating on rifampicin. Rif^R colonies were counted after 2 days of growth.

As the D521G oligo designed for *P. putida* KT2440 did not appear to produce recombinants, I designed a new oligo testing a D521P mutation for strains *P. protegens* Pf-5 and *P. protegens* CHA0 with the idea that perhaps the location of the mutation was more important than the specific residue aspartic acid was mutated to. This effectively changed the aspartic acid codon of GAC to the proline codon CCG, increasing the ability of the mutation to evade MMR as more nucleotides were changed. This point mutation also includes a bulkier side chain that I hypothesized would still negatively affect rifampicin binding, resulting in Rif^R.

With the *P. protegens* Pf-5 and *P. protegens* CHA0 strains, I used a D521P oligo across all 4 recombinases (Figures 2.4 and 2.5). In both strains, *E. coli* λ Red Beta resulted in the highest frequency of Rif^R colonies, ~1 x 10^{-4} and 5 x 10^{-4}, respectively. In *P. protegens* Pf-5, the next most efficient recombinase was RecT from *P. syringae* B728a, which had a frequency of Rif^R resistant colonies 10-fold lower than *E. coli* λ Red Beta. The *E. coli* RecT recombinase performed similarly to wildtype *P. protegens* Pf-5 when oligo was present, indicating low

activity, if any, by this recombinase. The W3 Beta recombinase resulted in no significant Rif^R activity *P. protegens* Pf-5, yet this recombinase performed well in *P. protegens* CHA0 at ~6 x 10^{-5} Rif^R/viable cells.

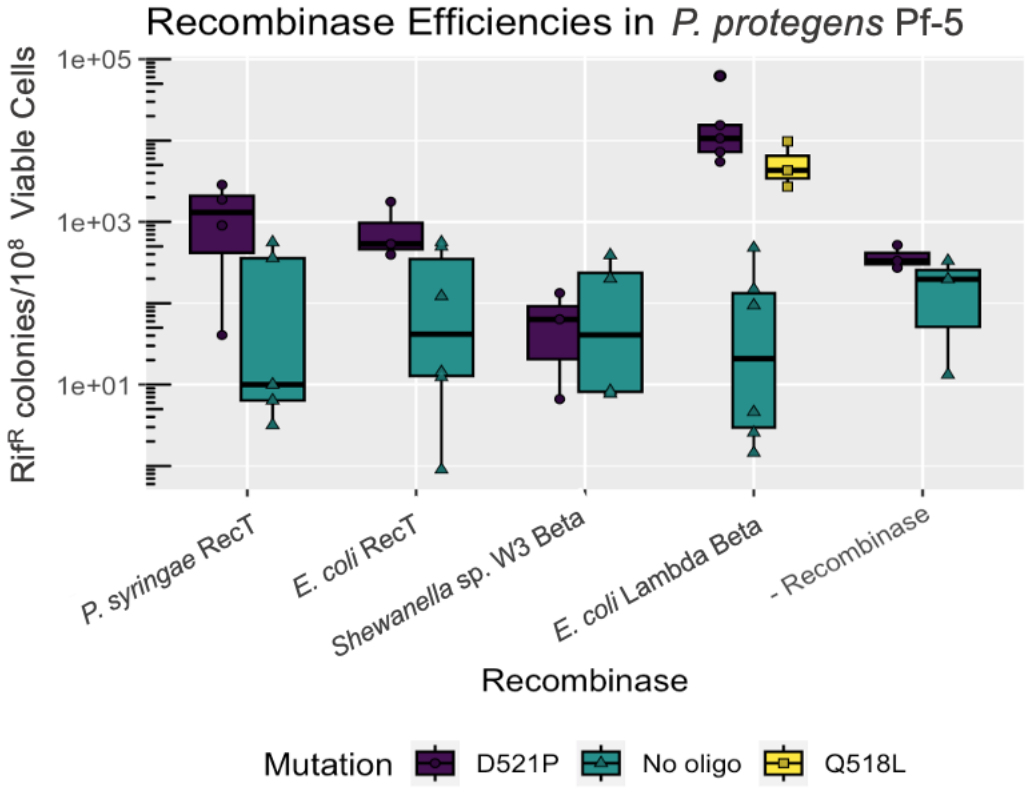

Figure 2.4. Recombineering of *rpoB* using *P. protegens* Pf-5. The effect of 4 different recombinases was examined in *P. protegens* Pf-5 using the D521P point mutation (16-bp mutagenic region). The Q518L mutation (4-bp mutagenic section) was tested solely in cells carrying *E. coli* λ Red Beta recombinase. 15 µg of oligo was electroporated into log phase cells, and the cell mixture recovered for 3.5 hours in LB before plating on rifampicin. Rif^R colonies were counted after 2 days of growth for the D521P mutation, and 4 days of growth for the Q518L mutation.

The Q518L recombinogenic oligo in both *P. protegens* strains resulted in an interesting delayed growth phenotype. When the Q518L oligo was used, an initial population of Rif^R mutants were present on the plate after 2 days of growth, followed by the recombineered Q518L colonies after 4 days of total growth (Appendix Figure 2.2). Every delayed colony screened using mutation-specific primers was found to carry the Q518L mutation (n=16), providing an additional method of decoupling inherent Rif^R from recombinase-induced Rif^R in these strains.

Further experiments are required to determine if the Q518L mutation results in a general growth rate defect in media without rifampicin.

In both *P. protegens* strains, the D521P oligo resulted in higher frequencies of rifampicin resistance compared to the Q518L mutation. This could be due to more stringent MMR requirements in these strains; perhaps the 4 bp standard to evade MMR developed in *E. coli* is not directly applicable to *Pseudomonas*. Additional experiments effectively swapping the mismatch length between these two point mutations may provide further insight to this inquiry, as well as testing additional oligos with lower or higher anticipated MMR evasion.

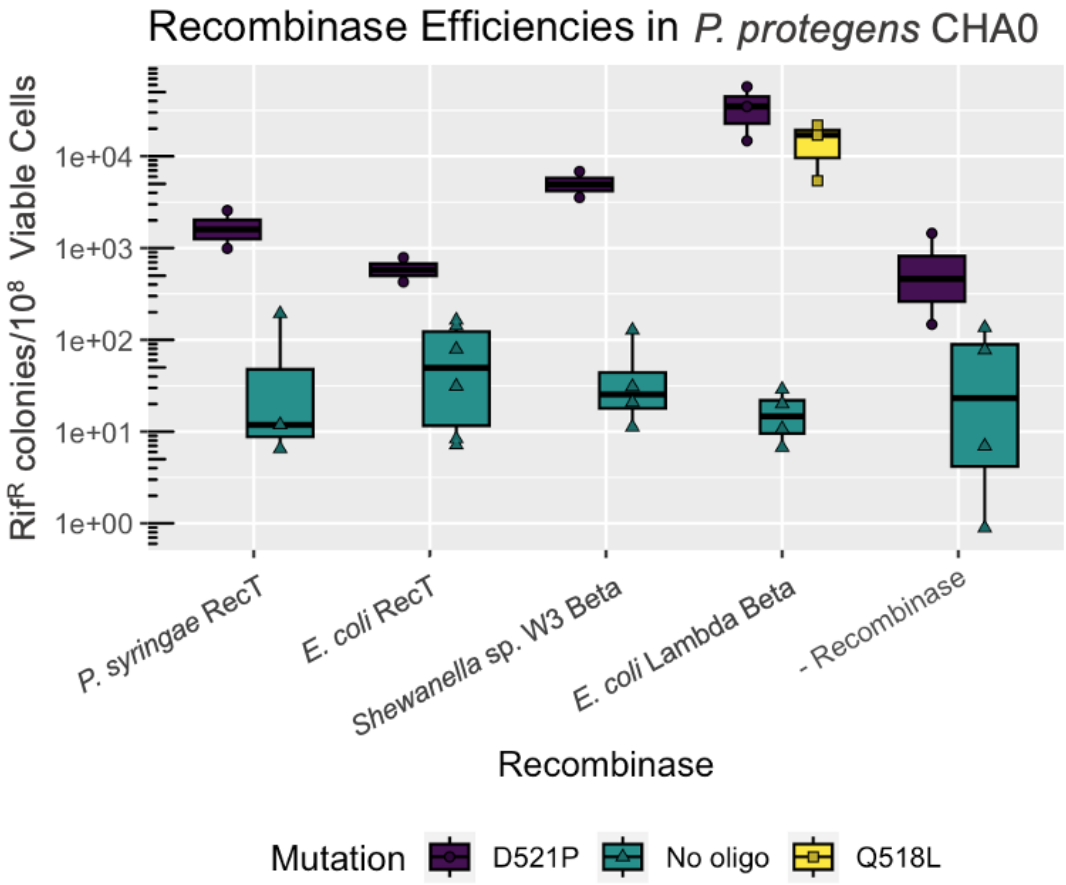

Figure 2.5. Recombineering of *rpoB* using *P. protegens* CHA0. The effect of 4 different recombinases was examined in *P. protegens* CHA0 using the D521P point mutation (16-bp mutagenic region). The Q518L mutation (4-bp mutagenic section) was tested solely in cells carrying *E. coli* λ Red Beta recombinase. 15 µg of oligo was electroporated into log phase cells, and the cell mixture recovered for 3.5 hours in LB before plating on rifampicin. Rif^R colonies were counted after 2 days of growth for the D521P mutation, and 4 days of growth for the Q518L mutation.

DNA substrate load improves recombineering frequencies

In an effort to test the effect of oligo amount on recombineering frequencies in *P. protegens* Pf-5, I used RecT from *P. syringae* pv. *syringae* B728a as it showed some activity in this strain but could be further improved (Figure 2.6). I tested 4 D521G ssDNA substrate load amounts of 0.3 µg, 3 µg, 15 µg, and 30 µg (with copy numbers of ~6 x 10^{12}, 6 x 10^{13}, 3 x 10^{14}, and 6 x 10^{14}, respectively). The recombineering efficiencies of RecT improved 3- to 5-fold for each increase in substrate, as did the controls without recombinase up to 15 µg, suggesting both that RecT performance and wildtype recombination are substrate concentration-dependent. This experiment also showed that wildtype *P. protegens* Pf-5 is capable of oligo recombination at lower levels without added recombinase. The frequency of Rif^R colonies in wildtype *P. protegens* Pf-5 does appear to saturate at higher amounts of oligo, suggesting an upper limit to recombinase-independent recombination frequencies.

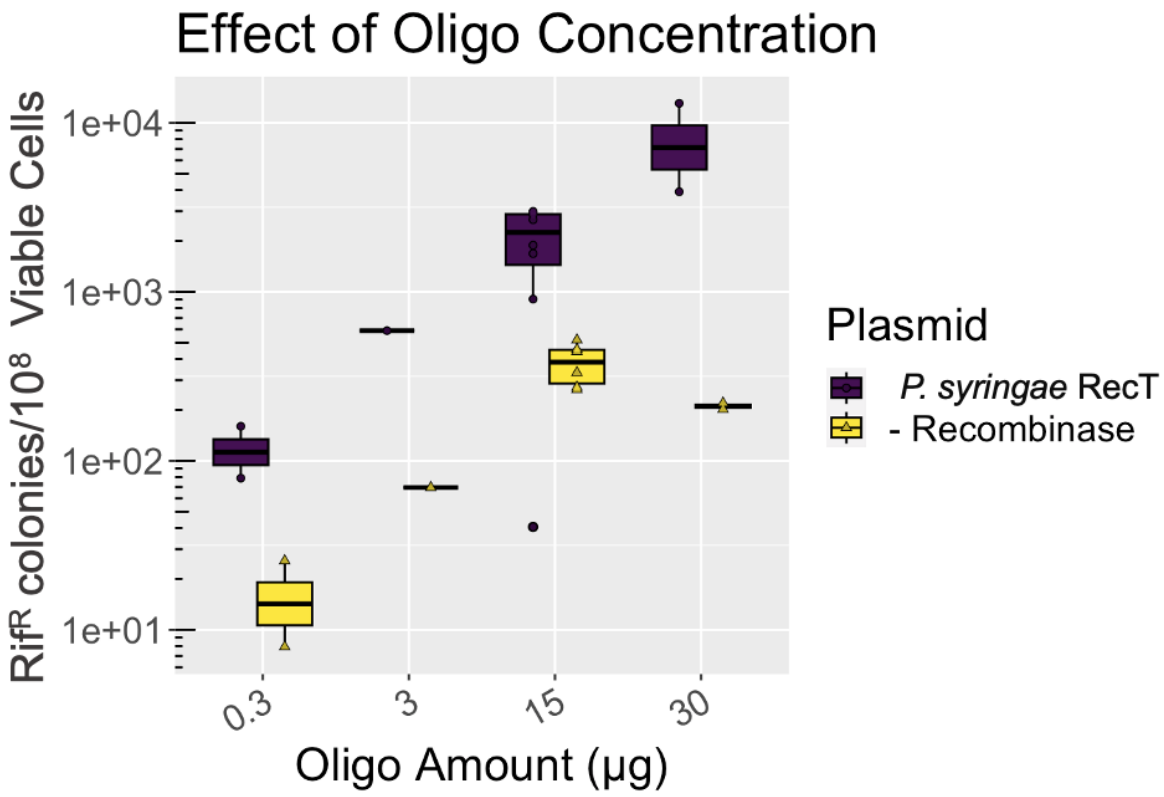

Figure 2.6. DNA substrate load on recombineering. The number of Rif^R colonies as a function of ssDNA substrate added in both wildtype *P. protegens* Pf-5 and with plasmid carrying constitutively expressed RecT from *P. syringae* pv. *syringae* B728a. Volume of D521P oligo added did not exceed 10 µL.

Effect of oligo protection on recombineering

To determine possible ways to improve recombineering in *P. protegens* Pf-5 beyond recombinase and ssDNA amount, I tested two methods of oligo protection: the use of phosphorothiolate bonds or the addition of *E. coli* λ Gam protein. Both methods have been used in other studies to prevent the degradation of oligos by endogenous nucleases. The addition of 4 5' phosphorothiolate bonds was shown to increase the frequency of Rif^R colonies when *P. syringae* RecT was used and in wildtype *P. protegens* Pf-5 by ~1.6 fold (Figure 2.7).

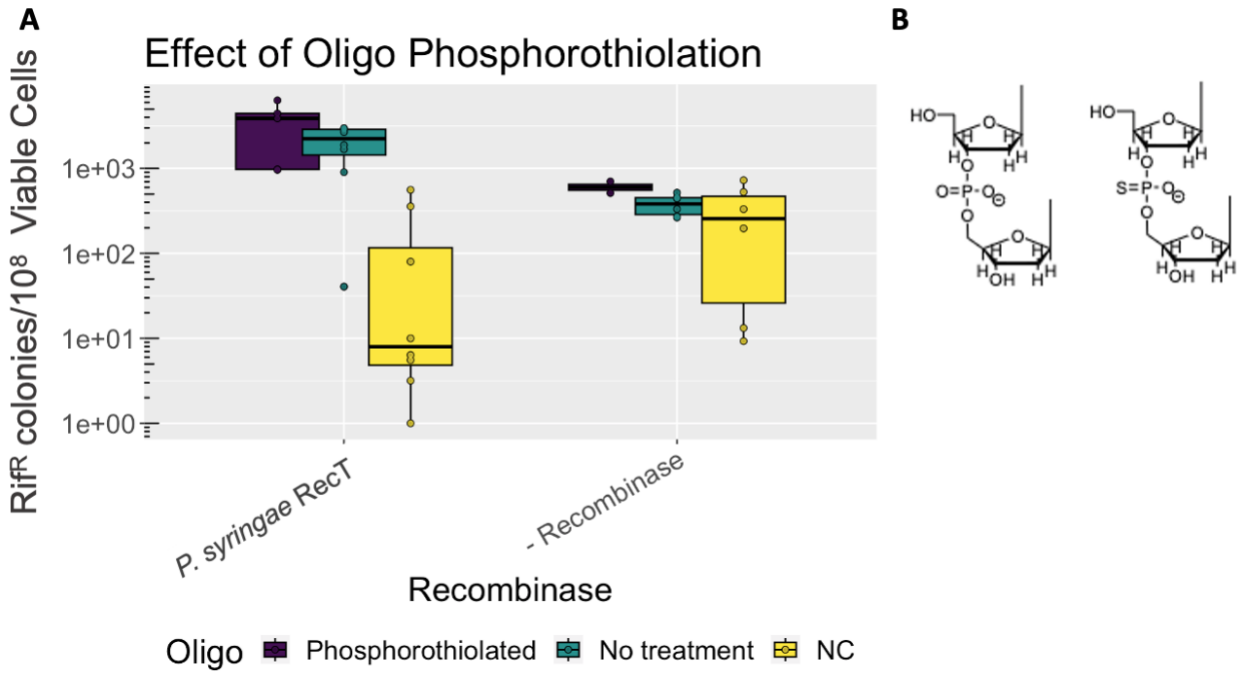

Figure 2.7. Effect of phosphorothiolate bonds on recombineering. (A) The addition of 4 5' phosphorothiolate bonds were tested using 15 µg of D521P oligo in *P. protegens* Pf-5 to protect from nuclease degradation. **(B)** Visualization of molecular distinction between the standard phosphodiester bond (left) and a nuclease-resistant phosphorothiolate bond (right). Images drawn using ChemDraw.

A second method to protect ssDNA substrate from degradation was by the addition of the protein Gam, from *E. coli* BL21DE3 λ Red phage, which has been shown to protect exogenous DNA from the RecBCD family of nucleases. I cloned the Gam protein downstream of RecT from *P. syringae* pv. *syringae* B728a under the same constitutive promoter to determine whether addition of Gam would improve Rif^R colony frequency in *P. protegens* Pf5 using the D521P mutation. It was found that addition of Gam did not result in higher recombineering frequencies using this experimental setup (Figure 2.8). Additional experiments would be required to

determine if Gam protein actually inhibits RecT recombinase function, or if the *E. coli* Gam does not seem to interact with *P. protegens* RecBCD nucleases.

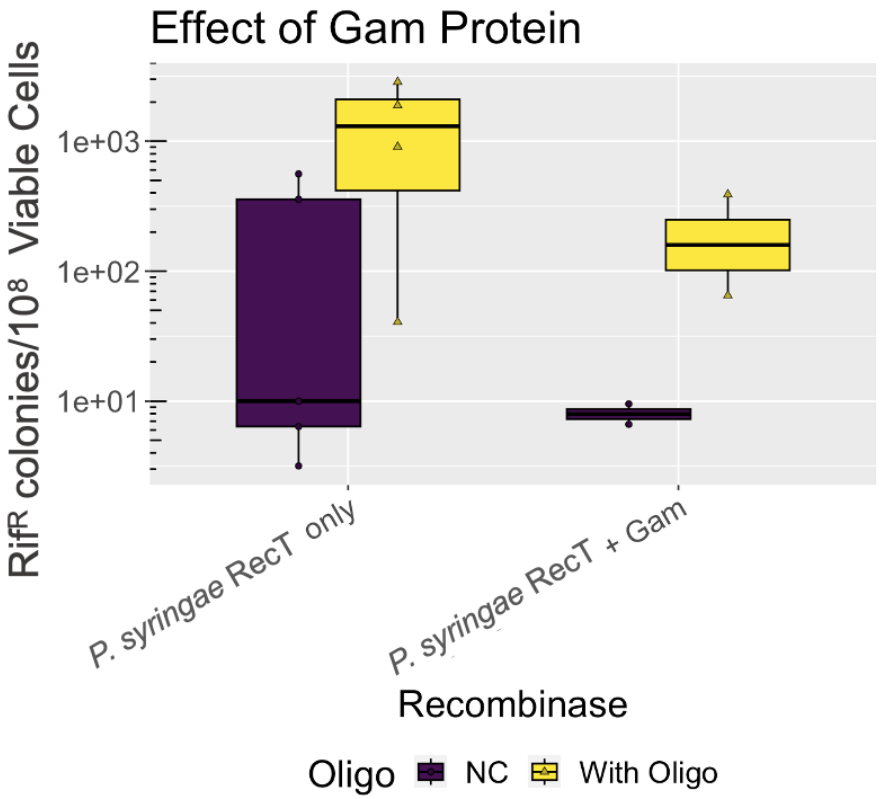

Figure 2.8. Addition of Gam protein to *rpoB* recombineering in *P. protegens* Pf-5. The *E. coli* BL21DE3 λ Red phage Gam CDS was constructed in a constitutively expressed operon downstream of RecT (*P. syringae* pv. *syringae* B728a). 15 µg of D521P oligo were electroporated into *P. protegens* Pf-5 strains harboring either plasmid expressing RecT only or RecT and Gam.

2.8 Discussion

This study provided a potential platform for further lines of inquiry in developing a robust recombineering system in environmental *Pseudomonas*. Here I directly compared several recombinases in their ability to mutate the *rpoB* gene using 2 native Rif^R point mutations as well as one experimentally discovered Rif^R point mutation. The efficiencies of recombineering observed in this study were some of the highest for two of the three *Pseudomonas* strains; however, reported recombineering efficiencies between our study and previous studies are difficult to directly compare. An additional layer of complexity is added to calculating recombineering efficiencies due to the non-standardized ways in which efficiency is measured and reported. The two ways to report efficiency can be more specifically represented by actual

and apparent efficiency (119). I define actual efficiency as the frequency of which a desired mutation was incorporated in the original population of cells, while the apparent efficiency is the frequency of desired mutation within the number of survivor clones after a recombineering attempt. The efficiency reported in this study is reported as total Rif^R colonies per 10^8 viable cells; however, this number includes the spontaneous Rif^R mutants as well as the recombinase dependent Rif^R clones. This is an estimate of the actual recombineering efficiency; I do not have sufficient data to report the apparent recombineering efficiency, although I hypothesize that the apparent recombineering efficiencies could be adequately estimated using the Q518L delayed growth phenotype in *P. protegens* Pf-5 and *P. protegens* CHA0 in future studies.

The difference between these two measures is more definitive when considering the ways in which apparent versus actual efficiency is improved. Actual efficiency is influenced by factors which affect the duration of oligo lifetime within a cell, including phosphorothiolate protection and removal of endogenous nucleases as well as the frequency of oligo incorporation, which is affected by the specific recombinase used, lagging strand targeting, and length of homology arms. Apparent efficiency is affected by counterselection strategies including Cas9. This measure affects total survivorship numbers but does not increase the actual frequency of recombination events within the original population. In this study I focused on testing different mechanisms of increasing actual efficiency by testing different recombinases and oligo protection methods with the use of phosphorothiolate bonds and the addition of Gam protein.

I observed evidence of host tropism within both *P. protegens* strains using RecT recombinases from two hosts with different evolutionary distances, as higher levels of oligo recombination frequency resulted from the more closely related *P. syringae* pv. *syringae* RecT. This host-tropism recombinase preference did not hold up when the λ Red Beta recombinase was used, as it resulted in the highest number of Rif^R colonies in all three strains tested. One possibility for this result is that λ Red Beta is more efficient than RecT in incorporating smaller oligonucleotides, as previous research in *Pseudomonas* has primarily used RecTE from *P. syringae* for insertions of larger dsDNA substrates (108, 142). The λ Red Beta-homolog Ssr T1E_1405 from *P. putida* DOT-T1E tested by Aparicio, et al. (130) was far more efficient at introducing small mutations than large ones, perhaps supporting the idea that RecT-like recombinases may be more efficient at introducing larger mutations into the genome, while λ Red Beta-like recombinases are more efficient at smaller mutations. Utilizing 90-mer

oligonucleotides may have caused a bias for λ Red Beta to outperform RecT in these *Pseudomonas* strains, so additional experiments testing the length of mutation size and oligo homology length may help to determine if these recombinases function optimally at different substrate DNA lengths.

Here I constitutively express different recombinases using a hypothesized medium strength promoter and RBS; however, the relative levels of recombinase expression may vary between strains and affect the availability of enzyme and thus the recombineering efficiency. Measuring expression levels under this constitutive system using GFP or another reporter gene may help to better quantify expression levels. Alternatively, expression levels of recombinase could also be investigated using SDS-PAGE to ensure expression. Further iterations of recombineering in this strain may additionally benefit from an inducible recombinase, as recombinase overexpression can lead to unintended off-target mutations and genome instability (92, 145). Overexpression of Gam protein is known to be toxic to cell survival, so inducible expression of this protein would also provide more information as to whether this addition is beneficial to recombineering in *Pseudomonas* (92, 121, 145).

The highest to-date recombineering efficiencies (that I are aware of) have been reported by Aparicio et al. using the *P. putida* KT2440 derivative strain EM42 (130, 146). Some of the higher efficiencies reported in this strain are likely due in part to the removal of nucleases in this strain (130, 147). The removal of *mutS* gene and dominant-negative expression of mutant *mutL* have been shown to improve recombineering effiencies in the *P. putida* KT2440 derivative strain as well as in *E. coli* (125, 126, 148). While making this genomic deletion does improve recombineering efficiency, it should be noted that Δ*mutS* can also cause genome instability. Making this deletion in *P. protegens* Pf-5 and CHA0 may also increase recombineering efficiencies; however, this may be detrimental to downstream applications as a biopesticide or as an industrial workhorse.

The ability of our different oligonucleotides to evade MMR machinery was investigated to an extent in this study, as total mutagenic lengths of 4 and 16 bp were tested. Additional experiments effectively swapping the mismatch length of the Q518L, D521G, and D521P may provide further insight if a relationship between these mismatch lengths and recombineering efficiencies truly exists.

An additional consideration for improving recombineering efficiency not tested in this work is codon optimization of recombinase genes. Codon-optimization generally improves expression when expressing non-native proteins in different organisms (149). Codon optimization of recombinases has been shown to both improve and hinder recombineering efficiencies and seems to be recombinase-specific, although this hypothesis is currently limited by lack of data (116, 117). Future experiments to determine if such a bias exists would be highly beneficial in the expansion of recombineering technologies to other non-model organisms.

Future directions for the results established in this study can be further utilized to implement a CRISPR/Cas9 counterselection tool. The delayed growth phenotype of Q518L mutants in *P. protegens* Pf-5 and *P. protegens* CHA0 provides a convenient background to test this counterselection strategy, as I could theoretically quantify Cas9 escapers after 2 days of growth and true recombinants after 4 days of growth. Cas9 counterselection has been shown to be effective in *P. putida* KT2440, which leads us to believe that this technology could also be used in *P. protegens* Pf-5 and *P. protegens* CHA0 strains (84, 146).

2.9 Conclusion

In this chapter I successfully perform recombineering in three environmental *Pseudomonas* strains by editing the *rpoB* gene. I designed specific point mutations based off of Rif^R mutant pools to introduce into the genome using four different recombinases. Recombineering efficiencies generated in this study ranged from 5×10^{-4} in *P. protegens* CHA0 to 2×10^{-5} in *P. putida* KT2440. Attempts to improve recombineering with a native *Pseudomonas* recombinase were performed and increased efficiencies up to 5-fold with higher substrate loads and 1.6-fold with phosphothiolate bonds. This work sets the foundation for more robust recombineering methodology to be established in the future with these strains, as well as providing interesting questions to be further explored.

2.10 Materials and Methods

Bacterial Strains

All strains and plasmids used in this work are listed in Table 2.4. *P. protegens* Pf-5, *P. protegens* CHA0, *P. fluorescens* Pf-01, *P. ogarae F113*, *P. chlororaphis* 30-84, *P. putida* KT2440 and *P. fluorescens* SBW25 were obtained from Lawrence Livermore National

Laboratory (Livermore, CA). LB medium (BD Difco™ Dehydrated Culture Media: LB Broth, Miller) was used to routinely culture bacteria. Solid media was supplemented with 1.5% w/v agar (Fisher BioReagents™ Agar, Powder / Flakes). Growth media was supplemented with kanamycin at a final concentration of 50 µg/mL for *P. protegens* Pf-5, *P. protegens* CHA0, *P. fluorescens* Pf-01, *P. ogarae F113*, *P. chlororaphis* 30-84, and the routine *E. coli* strains used for cloning and conjugation, while a concentration of 100 µg/mL was used for *P. putida* KT2440 and *P. fluorescens* SBW25. LB plates supplemented with rifampicin (50 µg/mL) were wrapped in foil to prevent photodegradation. Cultures were grown aerobically at 30˚C (*Pseudomonas sp.*) or 37˚C (*E. coli*) and shaken at 250 rpm.

Table 2.4. Strains and plasmids used in this work

Strain or plasmid	Description	Reference or source
UQ950	*E. coli* DH5α λ (pir) host for cloning	(Saltikov & Newman 2003)
GM2163	*E. coli* dam$^-$, dcm$^-$, CmR	CGSC#: 6581
JG3554	*E. coli* UQ950, pSIM5-oriT	Court Lab
JG3871	*E. coli* UQ950, pX2NRecT	Gralnick Lab
JG4130	*E. coli* UQ950, pX2W3Beta	Gralnick Lab
JG4326	*E. coli* GM2163, pX2Cas9	Gralnick Lab
JG4366	*P. protegens* CHA0	LLNL
JG4367	*P. protegens* Pf-5	LLNL
JG4368	*P. synxantha* 2-79	LLNL
JG4369	*P. fluorescens* Pf-01	LLNL
JG4371	*P. ogarae* F113	LLNL
JG4405	*P. fluorescens* SBW25	LLNL
JG4406	*P. putida* KT2440	LLNL
JG4408	*E. coli* UQ950, pBBR1-Prha-redγ-recTE (*P. syringae* B728a)	Yin Lab
JG4736	*P. protegens* Pf-5, pMK3a	This work
JG4737	*P. protegens* Pf-5, pMK3b	This work

JG4738	*P. protegens* Pf-5, pMK3c	This work
JG4739	*P. protegens* Pf-5, pMK3d	This work
JG4740	*P. protegens* CHA0, pMK3a	This work
JG4741	*P. protegens* CHA0, pMK3b	This work
JG4742	*P. protegens* CHA0, pMK3c	This work
JG4743	*P. protegens* CHA0, pMK3d	This work
JG4744	*P. putida* KT2440, pMK3a	This work
JG4745	*P. putida* KT2440, pMK3b	This work
JG4746	*P. putida* KT2440, pMK3c	This work
JG4747	*P. putida* KT2440, pMK3d	This work
JG4748	*P. protegens* Pf-5, pMK5a	This work
Plasmid		
pSIM5	pSC101 ori, cmR, P_{lac}, λ Red	Court Lab
pX2NRecT	pBBR1 ori, Km^R, P_{BAD}, RecT (*E. coli* MG1655 prophage)	Gralnick Lab
pX2W3Beta	pBBR1 ori, Km^R, P_{BAD}, W3 Beta (*S.* sp. W3-18-1)	Gralnick Lab
pX2Cas9	pBBR1 ori, Km^R, P_{BAD}, Cas9 (*S. pyogenes* M1 GAS)	Gralnick Lab
pBBR1-Prha-redγ-recTE (*P. syringae* B728a)	pBBR1 ori, Km^R, P_{rha}, redγ RecTE (*P. syringae* B728a)	Yin Lab
pMK1	pBBR1 ori, Km^R, P_{J23116} driven RecT (*E. coli* MG1655), P^{BAD} driven Cas9	This work
pMK3a	pBBR1 ori, Km^R, P_{J23116} driven RecT (*P. syringae* pv. syringae B728a)	This work
pMK3b	pBBR1 ori, Km^R, P_{J23116} driven RecT (*E. coli* MG1655)	This work

pMK3c	pBBR1 ori, Km^R, P_{J23116} driven W3Beta (*S.* sp. W3-18-1)	This work
pMK3d	pBBR1 ori, Km^R, P_{J23116} driven λ Red Beta (*E. coli* BL21DE3)	This work
pMK5a	pBBR1 ori, Km^R, P_{J23116} driven RecT (*E. coli* MG1655) and redγ in operon	This work

Table 2.5 Additional relevant sequences

Name	Sequence
Constitutive promoter P_{J23116}	TAGGTGTTGACAGCTAGCTCAGTCCTAGGGACTATG CTAGCTCTAGA
RBS Sp17	GAATTCTCAACTAACGGACAGGAGATATACATATG
T24 Terminator	AAAGCAAGCTGATAAACCGATACAATTAAAGGCTCCTTTTGGA GCCTTTTTTTTTGGAGATTTTCAACATGAAAAAATTATTATTTG ATGATCAGATAGCGGCGGGGAACTGCCAGACATCAAATAAAA CAAAAGGCTCAGTCGGAAGACTGGGCCTTTTGTTTTATCTGTTG TTTGTCGGTGA ACACTCTCCCG

Plasmid construction

Relevant sequences for plasmid construction are listed in Table 2.5 All primers used to construct plasmids are listed in Table 2.6. Primers were obtained from IDT (Coralville, IA). Cloning fragments were PCR amplified using Q5 polymerase 2X master mix (New England Biolabs). pX2gfp (if applicable). pMK1 was generated by Gibson assembly of the pX2Cas9 backbone with *E. coli* MG1655 RecT and a Gblock containing the T24 terminator sequence, P_{J23116} constitutive promoter, and RBS Sp17 from (86). AraC, P^{BAD}, and Cas9 were removed from pMK1 to generate pMK2. Recombinase genes were PCR amplified from JG3554 (*E. coli* BL21DE3 λ Red), JG3871 (*E. coli* MG1655 RecT), JG4130 (*S.* sp. W3-18-1), JG4408 (*P. syringae* B728a

RecT) with flanking BsaI sites for golden gate cloning into the pMK2 backbone downstream of RBS Sp17 to generate pMK3x plasmids. pMK4a was built using golden gate assembly to insert redγ downstream of RecT (*P. syringae* B728a) in pMK3a using BsaI enzyme (New England Biolabs).

Table 2.6 Primers used in this study.

Primer name	Sequence (5'-3') **Bold** indicates Gibson overhangs, Underline indicates BsaI sites for Golden Gate cloning	Purpose
Cloning Primers		
MK47F	**ACGGACAGGAGATATACAT**ATGACTAAGCAACCACCAATC	RecT (*E. coli* MG1655) F with Sp17 RBS overlap
MK47R	**CTTTTGACTTTCTGCATGGA**TTATTCCTCTGAATTATCGATTACACTG	RecT (*E. coli* MG1655) R with tonB terminator overlap
MK49F	**CGGTTTATCAGCTTGCTTT**GGTCAGGTATGATTTTTATGAC	F primer to linearize pX2Cas9 backbone for pMK1* cloning
MK49R	TCCATAGCAGAAAGTCAAAAG	R primer to linearize pX2Cas9 backbone for pMK1* cloning
MK58F	ggctacggtctcc*TCGT*CAACGAATTCAAGC	F primer to remove AraC from pMK1
MK62R	ggctacggtctcc*acga*TCATACCTGACCAAAGCAAG	R primer to remove AraC from pMK1
MK64F	ggctacggtctcc*ACAT*ATGACTAAGCAACCAC	F primer for RecT (*E. coli* MG1655) to make pMK3b

MK64R	ggctacggtctcc*ACAT*ATGACTAAGCAACCAC	R primer for RecT (*E. coli* MG1655) to make pMK3b
MK65F	ggctacggtctcc*ACAT*ATGGAAAAACCAAAGCTA	F primer for W3 Beta to make pMK3c
MK65R	ggctacggtctccTGGACTAAGAAGCTAAAGGCTG	R primer for W3 Beta to make pMK3c
MK69F	cggctacggtctctATGTATATCTCCTGTCCGTTAG	F primer for golden gate cloning under Sp17 RBS to make pMK3x
MK69R	catagaggtctcatccactagcatttAGTCAAAACCTCCGACCG	R primer for golden gate cloning under Sp17, overlap with tonB terminator to make pMK3x
MK72F	ggctacggtctcc*ACAT*ATGTCCGCAAGAAACGTT	F primer for RecT (*P. syringae*) to make pMK3a
MK72R	ggctacggtctcc*TGGA*TCATGCGGTTTCTCCG	F primer for RecT (*P. syringae*) to make pMK3a
MK74F	ggctacggtctcc*ACAT*ATGAGTACTGCACTCGCA	F primer for λ Red (*E. coli* BL21DE3) to make pMK3d
MK74R	ggctacggtctcc*TGGA*TCATGCTGCCACCTTCT	R primer for λ Red (*E. coli* BL21DE3) to make pMK3d
MK75F	cggctacggtctctATGTTCATGCGGTTTCTC	F primer to insert Gam downstream recombinase,

		into RecT (*P. syringae*) to make pMK5a
MK75R	catagaggtctcaTCCACTAGCATTTAGTC	R primer to insert Gam downstream recombinase, into tonB terminator to make pMK5a
Screening primers		
MK51F	CAGACGATAGCCAATGATTAGCTG	RecT (*E. coli* MG1655) mid-sequence to check pMK1 assembly
MK51R	CAGAGCTCAGTCGGAAGACTG	T24 terminator mid-sequence to check pMK1 assembly
pX2F	TAGAGCCTCGGTGAGTTTTC	F primer from Km^R to check insert size in pX2/MK backbone
pX2R	TAGACGAAGCGAGCCAG	F primer from Km^R to check insert size in pX2/MK backbone
rpoBF3	CAGACGAGAACCAGTTCC	Universal F primer from nucleotide 1394 in *rpoB* gene
rpoBR4	CAGAGACAGGAACACGAT	R primer from nucleotide 1822 in *rpoB* gene, works in *P. protegens* Pf-5, *P. protegens* CHA0, *P. chlororaphis* 30-84, *P. fluorescens* Pf-01, *P. ogarae* F113, *P. putida* KT2440
rpoBR5	CAGAGACAGGAATACGATCT	R primer from nucleotide 1822 in *rpoB* gene of *P. fluorescens* SBW25

rpoBmut F	CAGACCAGCTGTCACTTTT	F primer with Q518L *rpoB* mutation
rpoBmut F3	CAGAGTTTATGGGCCAAAATAA	F primer with D521G *rpoB* mutation in *P. putida* KT2440
rpoBmut F4	CAGATATGCCGCAAAATAATC	F primer with D521P *rpoB* mutation in *P. protegens* Pf-5, *P. protegens* CHA0

Screening for recombineering target

As recombineering frequencies change based on the length and type of mutation introduced, I wanted to maximize the expected recombineering frequencies by introducing a small yet screenable mutation into the *Pseudomonas* genome. This required the utilization of a positive selection-based recombineering target. One such target is the *rpoB* gene, in which specific point mutations can confer resistance to the antibiotic rifampicin. Based on the characterization of rifampicin resistant mutations performed in *P. aeruginosa* and *P. putida* by Jastenko et al., I hypothesized that Rif^R mutations in our selection of *Pseudomonas* species may not be uniform in resistance strength or identity. To identify Rif^R mutations in our group of Pseudomonads, overnight cultures of each strain were plated on 50 μg/mL or 100 μg/mL rifampicin and incubated at 30˚C until colonies formed (36-48 hours). Primers were designed to amplify clusters I and II of the *rpoB* gene described in (144), where rifampicin is known to bind and most Rif^R mutations occur. This 400 bp fragment within the *rpoB* gene of 10 Rif^R mutants for each strain grown on 50 μg/mL rifampicin was PCR amplified and Sanger sequenced by ACCT, Inc (Wheeler, IL) to identify point mutations resulting in rifampicin resistance. Sequence outputs were aligned using EMBL-EBI MUSCLE (**MU**ltiple **S**equence **C**omparison by **L**og-**E**xpectation) tool.

Table 2.7. ssDNA oligonucleotides used for chromosomal recombineering.

Name	Sequence
Pf5/CHA0 Q518L-lag-40	CTGCGGCAGTGAAAGAGTTCTTCGGTTCCAGCCAGCTGTC**AC<u>TT</u>**TT CATGGACCAGAACAACCCGCTGTCCGAGATCACCCACA

KT2440-Q518L-lag-40	CGGCAGCGGTGAAAGAGTTCTTCGGTTCCAGCCAGCTGTC**AC**<u>**TT**</u>TTCATGGACCAGAACAACCCTCTCTCGGAGATTACCCACA
Pf5 D521P-lag-40	CAGTGAAAGAGTTCTTCGGCTTCCAGCCAGTCTGTCCCAGTT<u>**T**ATG**C** **CG**CA**A**A**T**AA**T**</u>CCGCTGTCCGAGATCACCCACAAGCGCCGTGTTTC TGCAC
CHA0-D521P-lag-40	CAGTGAAAGAGTTCTTCGGCTTCCAGCCAGTCTGTCCCAGTT<u>**T**ATG **CCG**CA**A**A**T**AA**T**</u>CCGCTGTCCGAGATCACCCACAAGCGTCGTGTTT CTGCAC
KT2440-D521G-lag-40	AGCGGTGAAAGAGTTCTTCGGTTCCAGCCAGCTGTCCCAGTT<u>**T**A TG**GGC**CA**A**AA**T**</u>AACCCTCTCTCGGAGATTACCCACAAGCGCC GCGTCTCCG

Oligonucleotide design

Recombinogenic oligonucleotides are listed in Table 2.7. Oligonucleotides were obtained as 250 nmole oligos from IDT (Coralville, IA). Oligos were resuspended in water to a final concentration of 100 μM. They were designed to introduce single amino acid point mutations within the *rpoB* gene resulting in rifampicin resistance or to encode a frameshift and premature stop codon in the *lacZ* gene. Point mutations were flanked by silent mutations to result in a total mutagenic segment of 4-10 bp to evade MMR. Criteria to design oligonucleotides were explored in (130, 132] and were used as guidelines for this work. 40 bp of homology flanked each side of the mutagenic segment to generate recombinogenic oligonucleotides of 90-100 nt in length. The mFold application via UNAFold (http://www.unafold.org/mfold/applications/dna-folding-form.php) was used to calculate DNA folding energies using a folding temperature of 30˚C and the default settings (150)(151). According to (132), optimal folding temperatures recombinogenic oligonucleotides in *E. coli* are above -20 kcal/mol, with a peak at about -12.5 kcal/mol. The (130) paper tested recombinogenic oligonucleotides with a range of -13 to -16 kcal/mol. In this work a range of -7 to -14 kcal/mol was used. When indicated, 4 phosphorothiolate bonds were introduced at the 5' end of the oligonucleotide to investigate the effect of DNA protection against endonucleases.

Recombineering in Pseudomonas

Plasmids pMK3a, b, c, or d or pMK5a were transformed into *P. putida* KT2440, *P. protegens* Pf-5, or *P. protegens* CHA0 via electrotransformation. single colonies were inoculated into 3 mLs of LB and grown overnight at 30˚C and 250 rpm. Cultures were diluted to an OD600 ~ 0.085 and grown in the same conditions until they reached an OD of 0.4-0.6, as downstream applications would require log phase cells. 4 mLs of culture were used per replicate. Cells were harvested by centrifugation at 10,000 rpm for 1 minute. Cell pellets were gently washed three times by resuspension in 1 mL of 1 M sorbitol (pH 7.6) for the *P. protegens* strains or 300 mM sucrose for *P. putida* KT2440. Each wash was followed by centrifugation under the same conditions as above, decanting the supernatant each time. After the final wash, cells were resuspended in a final volume of 60-70 µL and 5 µL of 100 µM recombinogenic oligo was mixed into the cell suspension (unless testing effect of oligo concentration, in which 0.1, 1, 5, and 10 µL of oligo were tested). The cell suspension was transferred into a 0.1 cm cuvette (Bio-Rad: Gene Pulser Cuvette, E. coli Pulser Cuvette) and a pulse was applied (settings: 25 µF; 200 Ω; 1.2 kV (unless otherwise specified) on a Bio-Rad GenePulserXcell™; Bio-Rad). 1 mL of LB was added, and cells were transferred to a 2 mL Eppendorf tube to recover at 30˚C and 250 rpm for 3.5 hours to allow time for membrane repair and oligo integration. 10X dilutions were plated onto LB rifampicin (50 µg/mL) as well as LB and incubated at 30˚C. Colonies were counted after 2 days of growth except in the case of *P. protegens* Pf-5 and *P. protegens* CHA0 when the Q518L oligo was used, in which colonies were counted after 4 days of incubation. All experiments included at least 2 biological replicates. Presence of mutation was confirmed via mutation specific PCR primers rpoBF, rpoBF3, and rpoBF4 and reverse universal primer rpoBR4. Presence of recombineered colony mutations were also confirmed using Sanger sequencing as discussed above from PCR with primers rpoBF3 and rpoBR4.

REFERENCES

1. Partensky, F, Garczarek, L. *Prochlorococcus*: advantages and limits of minimalism. *Ann Rev Mar Sci*, 2:305-331.
2. Jain, A, Gralnick, JA. (2020) Evidence for auxiliary metabolism anaerobic metabolism in obligately aerobic *Zetaproteobacteria*. *ISME J*, 14(4): 1057–1062.
3. Podile, A.R., Kishore, G.K. (2007). Plant growth-promoting rhizobacteria. In: Gnanamanickam, S.S. (eds) Plant-Associated Bacteria. Springer, Dordrecht. 195-230.
4. Silby, M., et al. (2011). *Pseudomonas* genomes: diverse and adaptable. *FEMS Microbiol Rev*, 35(4): 652-680.
5. Keswani, C, et al. (2020). Antimicrobial secondary metabolites from agriculturally important bacteria as next-generation pesticides. *Appl. Micro. and Biotechn.*, (104): 1013-1034.
6. Schalk I, Rigouin C, Godet J. (2020). An overview of siderophore biosynthesis among fluorescent Pseudomonads and new insights into their complex cellular organization. *Eviro. Microbiol.* 22(4):1447-1466.
7. Wang D, Yu JM, Pierson LS, Pierson EA. (2012). Differential regulation of phenazine biosynthesis by RpeA and RpeB in *Pseudomonas chlororaphis* 30-84. *Microbiology*, 158(7): 1745-1757.
8. Gouda, S, Kerry, RG, Das, G, Paramithios, S, et al. (2018). Revitalization of plant growth-promoting rhizobacteria for sustainable development in agriculture. *Microbiol. Research.* 206:131-140.
9. Humphris, SN, Bengough, AG, Griffiths, BS, Kilham, K, et al. (2005) Root cap influenes root colonization by *Pseudomonas fluorescens* SBW25 on maize. *FEMS Microbiol Ecol,* 54(1): 123-130.
10. Chojnacka, K, Moustakas K, Witek-Krowiak. (2020) Bio-based fertilizers: a practical approach to a circular economy. *Bioresour Technol.*, 295: 122223.
11. Glare, TR, Gwynn, RL, Moran-Diez, ME. (2016) Development of biopesticides and future opportunities. *Methods Mol Biol.*, 1477: 211-221.
12. Tabassum, B, Khan, A, Tariq, M, Ramzan, M, et al. (2017) Bottlenecks in commercialization and future prospects of PGPR. *Appl Soil Ecology*, 121:102-117.
13. Palleroni, N. (2010). The *Pseudomonas* story. *Environ. Micro.*, 12(6): 1377-1383.

14. Kersters, K, Ludwig, W, Vancanneyt, M, De Vos, P, et al. (1996). Recent changes in the classification of the Pseudomonads: an overview. *System. Appl. Microbiol.*, 19: 465-477.
15. Özen, A, Ussery, D. (2012). Defining the *Pseudomonas* genus: where do I draw the line with *Azotobacter*? *Microbial Ecology.* 63(2):239-248.
16. Shanahan, P, O'Sullivan, DJ, Simpson, P, Glennon, JD, O'Gara F. (1992) Isolation of 2,4-Diacetylphloroglucinol from a fluorescent pseudomonad and investigation of physiological parameters influencing its production. *Appl. And Environ. Microbiol.* 58(1): 353-358.
17. Howell, CR, Stipanovic, RD. (1979) Control of *Rhizoctonia solani* on cotton seedlings with *Pseudomonas fluorescens* and with an antibiotic produced by the bacterium. *Phytopathology*, 69:480-482.
18. Villacieros M, Power B, Sánchez-Contreras M, Lloret J, et al. (2003) Colonization behaviour of *Pseudomonas fluorescens* and *Sinorhizobium meliloti* in the alfalfa (*Medicago sativa*) rhizosphere. *Plant Soil*. 251 (1): 47-54.
19. Stanier, R., Palleroni, N., and Doudoroff, M. (1966) The aerobic Pseudomonads: a taxonomic study. *J. Gen. Microbiol.,* 43: 159-271.
20. Redondo-Nieto, M., Barret, M, Morrisey, J, Germaine K, et al. (2013). Genome sequence reveals that *Pseudomonas fluorescens* F113 possesses a large and diverse array of systems for rhizosphere function and host interaction. *BMC Genomics*, 14(54).
21. Fernàndez, M., et al. (2013). In vivo gene expression of *Pseudomonas putida* KT2440 in the rhizosphere of different plants. *Microb. Biotechnol.* 6(3):307-313.
22. Pierson, LS, III & Thomashow, LS. (1992). Cloning and heterologous expression of the phenazine biosynthetic locus from Pseudomonas aureofaciens 30-84. Mol Plant Microbe Interact 5, 330– 339.
23. Mezaache-Aichour S, Guechi A, Nicklin J, Drider D, Prevost H (2012) Isolation, identification and antimicrobial activity of pseudomonads isolated from the rhizosphere of potatoes growing in Algeria. *J Plant Pathol*., 94:89–98.
24. Mazzola, M, Fujimoto, DK, Thomashow, LS, Cook, RJ. (1995). Variation in sensitivity of *Gaeumannomyces graminis* to antibiotics produced by fluorescent *Pseudomonas* spp. and effect on biological control of take-all of wheat. *Appl. and Environ. Microbiol.* 61: 2554-2559.

25. Paulsen, IT, Press, CM, Ravel, J, Kobayashi, DY, et al. (2005) Complete genome sequence of the plant commensal *Pseudomonas fluorescens* Pf-5. *Nature*, 23(7): 873-878.
26. Gross, H, Stockwell, VO, Henkels, MD, Nowak-Thompson, B, et al. (2007). The genomisotopic approach: a systematic method to isolate products of orphan biosynthetic gene clusters. Chemistry & Biology, 14, 53–63.
27. Howell, CR. Stipaniovic, RD. (1980) Suppression of *Pythium ultimum*-induced damping-off of cotton seedlings by *Pseudomonas fluorescens* and its antibiotic, pyoluteorin.
28. Nowak-Thompson B, Gould SJ, Kraus J, Loper JE. (1994) Production of 2,4-diacetylphloroglucinol by the biocontrol agent *Pseudomonas fluorescens* Pf-5. *Can. J. Microbiol.* 40:1064–1066.
29. Loper, J, Henkels, M, Shaffer, B, Valeriote, F, Gross, H. (2008) Isolation and identification of rhizoxin analogs in *Pseudomonas fluorescens* Pf-5 by genome mining strategy. *Appl. Environ. Microbiol.* 74(10):3085-3093.
30. Pfender, W., Kraus, J., Loper, J. (1993). A genomic region from *Pseudomonas fluorescens* Pf-5 required for pyrrolnitrin production and inhibition of Pyrenophora tritici-repentis in wheat straw. *Phytopathology* 83:1223-1228.
31. Lim, C. et al. (2016) Disruption of transporters affiliated with enantio-pyochelin biosynthesis gene gluster of *Pseudomonas protegens* Pf-5 has pleiotropic effects. *PLoS One 11*(7): e0159884.
32. Jousset, A, Schuldes, J, Keel, C, Maurhofer, M, et al. (2014) Full-genome sequence of the plant growth-promoting bacterium *Pseudomonas protegens* CHA0. *Genome Announc*. 2(2): e00322-14.
33. Smits, T, Rezzonico, F, Frasson, D, Vesga, P, et al. (2019) Updated Genome Sequence and annotation for the full genome of Pseudomonas protegens CHA0. *Microbiol Resour Announc* 8:e01002-19.
34. Stutz, EW, Défago, G, Kern, H. (1986) Naturally occurring fluorescent Pseudomonads involved in suppression of black root rot of tobacco. *Phytopathology*, 76:181-185.
35. Maurhofer, M, Hase, C, Meuwly, P, Métrauz, JP, et al. (1994) Induction of systemic resistance of tobacco to tobacco necrosis virus by the root-colonizing *Pseudomonas fluorescens* strain CHA0: Influence of the *gacA* gene and of pyoverdine production. *Phytopathology*, 84:139-146.

36. Ramette, A, Frapolli, M, Fischer-Le Saux, M, Gruffax, C, et al. (2011) *Pseudomonas protegens* sp. nov., widespread plant-protecting bacteria producing the biocontrol compounds 2,4-diacetylphloroglucinol and pyoluteorin. *Systematic and Applied Microbiol*. 34: 180-188.
37. Laville, J, Blumer, C, Von Schroetter, C, Gaia, V, et al. (1998). Characterization of the *hcnABC* gene cluster encoding hydrogen cyanide synthase and anaerobic regulation by ANR in the strictly aerobic biocontrol agent *Pseudomonas fluorescens* CHA0. *Journal of Bacteriology*, 180:3187–3196.
38. Garrido-Sanz, D., Redondo-Nieto, M., Martin, M., Rivilla, R. (2021) Comparative genomics of the *Pseudomona corrugata* subgroup reveals high species diversity and allows the description of *Pseudomonas ogarae* sp. nov. *Microb. Genom.*, 7(6): 00593.
39. Cronin D, Moenne-Loccoz T, Fenton A, Dunne C, et al. (1997) Ecological interaction of a biocontrol *Pseudomonas fluorescens* strain producing 2,4-diacetylphloroglucinol with the soft rot potato pathogen *Erwinia carotovora subsp. atroseptica*. *FEMS Microbiol Ecol.,* 23(2):95–106.
40. Oteino, N, Lally, RD, Kiwanuka, S, Lloyd, A, et al. (2015) Plant growth promotion induced by phosphate solubilizing endophytic *Pseudomonas* isolates. *Front. Microbiol.*, 6:745.
41. Aarons S, Abbas A, Adams C, Fenton A, O'Gara F. (2000) A regulatory RNA (PrrB RNA) modulates expression of secondary metabolite genes in *Pseudomonas fluorescens* F113. J Bacteriol. 182 (14): 3913-3919.
42. Lewis TA, Leach L, Morales S, Austin PR, et al. (2006) Physiological and molecular genetic evaluation of the dechlorination agent, pyridine-2,6-bis(monothiocarboxylic acid) (PDTC) as a secondary siderophore of *Pseudomonas*. *Environ Microbiol.,* 6(2):159–169.
43. Silby, MW, Cerdeño-Tárraga, AM, Vernikos, GS, Giddens, SR, et al. (2009) Genomic and genetic analyses of diversity and plant interactions of *Pseudomonas fluorescens*. *Genome Biol.*, 10(5):R51.
44. Compeau, G, Al-Achi, BJ, Platsouka, E, Levy, SB. (1988) Survival of rifampin-resistant mutants of *Pseudomonas fluorescens* and *Pseudomonas putida* in soil systems. *Appl. Environ. Microbiol*., 54:2432–2438.

45. Ravel, J, Cornelis, P. (2003) Genomics of pyoverdine-mediated iron uptake in pseudomonads. *Trends Microbiol.,* 11(5):195-200.
46. Monds, RD, Newell, PD, Schwartzman, JA, O'Toole, GA. (2006) Conservation of the Pho regulon in *Pseudomonas fluorescens* Pf0-1. *Appl. Eviron. Microbiol.*, 72(3):1910-1924.
47. Bailey, MJ, Thompson, IP (1992). Detection systems for phyllosphere Pseudomonads. *Genetic Interactions Between Microorganisms in the Natural Environment,* Pergamon Press, Oxford, UK.
48. Moon, CD, Zhang, XX, Matthijs, S, Schäfer, M, et al. (2008) Genomic, genetic and structural analysis of pyoverdine-mediated iron acquisition of the plant growth-promoting bacterium *Pseudomonas fluorescens* SBW25. *BMC Microbiol*, 8:7.
49. De Brujin, I, de Kock, MJD, Yang, M, de Waard, P, et al. (2007) Genome-based discovery, structure prediction and functional analysis of cyclic lipopeptide antibiotics in *Pseudomonas* species. *Molecular Microbiol.* 63(2):417-428.
50. Trippe, K, McPhail, K, Armstrong, D, Azvedo, M, et al. (2013). *Pseudomonas fluorescens* SBW25 produces furanomycin, a non-proteinogenic amino acid with selective antimicrobial properties. *BMC Microbiol.* 13(111).
51. Loper, J, Hassan, KA, Mavrodi, DV, Davis II, EW, et al. (2012) Comparative genomics of plant-associated *Pseudomonas* spp.: insights into diversity and inheritance of traits involved in multitrophic interactions. *PLoS Genet.*, 8(7): e10022784.
52. Weller, DM, Cook, RJ. (1983) Suppression of take-all of wheat by seed treatments with fluorescent pseudomonads. *Phytopathology*, 73:463-469.
53. Delaney SM, Mavrodi DV, Bonsall RF, Thomashow LS. (2011) *phzO*, a gene for biosynthesis of 2-hydroxylated phenazine compounds in *Pseudomonas aureofaciens* 30–84. *J. Bacteriol.,* 183(1):318–327.
54. Chen, Y, Shen, X, Peng, H, Hu, H, et al. (2015) Comparative genomic analysis and phenazine production of *Pseudomonas chlororaphis*, a plant growth-promoting rhizobacterium. *Genom Data*, 4:33-42.
55. Regenhardt, D, Heuer, H, Heim, S, Fernandez, DU, et al. (2002). Pedigree and taxonomic credentials of *Pseudomonas putida* strain KT2440. *Environ. Microbiol.* 4(12): 912-915.

56. Nelson, KE, Weinel, C, Paulsen IT, Dodson, RJ, et al. (2002). Complete genome sequence and comparative analysis of the metabolically versatile *Pseudomonas putida* KT2440. *Eviron. Microbiol.* 4(12): 799-808.
57. Belda, E, van Heck, RGA, Lopez-Sanchez, MJ, Cruveiller, S, et al. (2016). The revisited genome of *Pseudomonas putida* KT2440 enlightens its value as a robust metabolic chassis. *Environ. Microbiol.* 18(10): 3403-3424.
58. Nakazawa, T. (2002) Travels of a *Pseudomonas*, from Japan around the world. *Eviron. Microbiol.* 4(12): 782-786.
59. An, R, Moe, LA. (2016) Regulation of pyrroloquinoline quinone-dependent glucose dehydrogenase activity in the model rhizosphere-dwelling bacterium *Pseudomonas putida* KT2440. *Appl Environ Microbiol*, 82(16):4955-4964.
60. Wu, X, Monchy, S, Taghavi, S, Zhu, W, et al. (2011). Comparative genomics and functional analysis of niche-specific adaptation in *Pseudomonas putida*. *FEMS Microbiol. Reviews*, 35(2):299-323.
61. Costa-Gutierrez, SB, Lami, MJ, Caram-Di Santo, MC, Zenoff, AM, et al. (2020). Plant growth promotion by *Pseudomonas putida* KT2440 under saline stress: role of eptA. *Appl. Microbiol. Biotechnol.* 104(10):4577-4592.
62. Nesemann, K, Braus-Stromeyer, SA, Thuermer, A Daniel, R, et al. (2015) Draft genome sequence of the phenazine-producing *Pseudomonas fluorescens* 2-79. *Genome Announc*, 26(3):e00130-15.
63. Mavrodi, D, Ksenzenko, VN, Bonsall, RF, Cook, RJ, et al. (1998) A seven-gene locus for synthesis of phenazine-1-carboxylic acid by *Pseudomonas fluorescens* 2-79. *J Bacteriol*. 180(9): 2541-2548.
64. Hamdan, H, Weller, DM, Thomashow, LS. (1991) Relative importance of fluorescent siderophores and other factors in biological control of *Gaeumannomyces graminis* var. *triciti* by *Pseudomonas fluorescens* 2-79 and M4-80R. *Appl Microbiol Biotechnol*, 57(11):3270-3277.
65. Slininger, PJ, Burkhead, KD, Schisler, DA, Bothast, RJ. (1999) Isolation, identification, and accumulation of 2-acetamidophenol in liquid cultures of the wheat take-all biocontrol agent *Pseudomonas fluorescens* 2-79. *Appl Microbiol Biotechnol*, 54:376-381.

66. de Souza JT, Weller DM, Raaijmakers JM. (2003) Effect of 2,4-diacetylphloroglucinol on *Pythium*: cellular responses and variation in sensitivity among propagules and species. *Phytopathology*, 93:966–975.
67. Islam MT, Fukushi Y. (2010) Growth inhibition and excessive branching in *Aphanomyces cochlioides* induced by 2,4-diacetylphloroglucinol is linked to disruption of filamentous actin cytoskeleton in the hyphae. *World J Microbiol Biotechnol*, 26:1163–1170.
68. Balthazar, C, St-Onge, R, Léger, G, Lamarre, SG, et al. (2022) Pyoluteorin and 2,4-diaacetylphloroglucinol are major contributors to *Pseudomonas protegens* Pf-5 biocontrol against *Botrytis cinereal* in cannabis. *Front. Microbiol.,* 13:945498.
69. Pellicciaro, M, Padoan, E, Lione, G, Celi, L, et al. (2022) Pyoluteorin produced by biocontrol agent *Pseudomonas protegens* is involved in the inhibition of *Heterobasidion* species present in Europe. *Pathogens*, 11(4):391.
70. Loper, JE, Henkels, MD, Rangel, LI, et al. (2016) Rhizoxin analogs, orfamide A and chitinase production contribute to the toxicity of *Pseudomonas protegens* strain Pf-5 to *Drosophila melanogaster*. *Environ. Microbiol.* 18(10): 3509-3521.
71. Tankara, K, Tamaki, M, Watanabe, S. (1969) Effect of furanomycin on the synthesis of isoleucyl-tRNA. *Biohhim. Biophys. Acta,* 195:244-245.
72. Ramette, A, Frapolli, M, Défago, G, Moënne-Loccoz, Y. (2003). Phylogeny of HCN synthase-encoding *hcnBC* genes in bioconfrol fluorescent Pseudomonads and its relationship with host plant species and HCN synthesis ability. *MPMI,* 16(6):525-535.
73. Cook, SD. (2019) An historical review of phenylacetic acid. *Plant Cell Physiol*, 60(2): 243-254.
74. Keswani, C, Singh, SP, Cueto, L, García-Estrada, C, et al. (2020) Auxins of microbial origin and their use in agriculture. *Appl Microbiol Biotechnol*, 104:8549-8565.
75. Shutter, MC, Akhondi, H. (2022) Tetracycline: StatPearls. Treasure Island (FL). 2022 Jan-.
76. Oong GC, Tadi P. Chloramphenicol. (2022). Chloramphenicol: StatPearls. Treasure Island (FL). 2022 Jan-.
77. Peechakara, BV, Basit, H, Gupta, M. (2022). Ampicillin: StatPearls. Treasure Island (FL). 2022 Jan-.

78. Suzuki, J, Kunimoto, T, Hori, M. (1970) Effects of kanamycin on protein synthesis: inhibition of elongation of peptide chains. *J. Antibiotics*, 23(2):99-101.
79. Fernández, M, Conde, S, de la Torre, J, Molina-Santiago, C, et al. (2012) Mechanisms of resistance to chloramphenicol in *Pseudomonas putida* KT2440. *Antimicrob Agents Chemother.* 56(2): 1001-1009.
80. Waters, M, Tadi, P. (2022) Streptomycin: StatPearls. Treasure Island (FL). 2022 Jan-.
81. Yu, F, Jing, X, Li, X, Wang, H et al. (2019) Recombineering *Pseudomonas protegens* CHA0: An innovative approach that improves nitrogen fixation with impressive bactericidal potency. Micro Research 218 58-65.
82. Khan, S, Mavrodi, DV, Jog, GJ, Suga, H, et al. (2005) Activation of the phz operon of Pseudomonas fluorescens 2-79 requires the LuxR homolog PhzR, N-(3-OH-hexanoyl)-L-homosering lactone produced by the LuxI homolog PHzI, and a cis-active phz box. J Bacteriol. 187(8): 6517-6527.
83. Choi, KH, Kumar, A, Schweizer, HP. (2006) A 10-min method for preparation of highly electrocompetent *Pseudomonas aeruginosa* cells: Application for DNA fragment transfer between chromosomes and plasmid transformation. *J. Microbiol. Methods*, 64(3): 391-397.
84. Wu Z, Chen Z, Gao X, Li J, et al. (2019) Combination of ssDNA recombineering and CRISPR-Cas9 for *Pseudomonas putida* KT2440 genome editing. *Appl. Microbiol. Biotechnol.*, 103:2783-2795.
85. Sathesh-Prabu, C, Tiwari, R, Kim, D, Kuk Lee, S. (2021) Inducible and tunable gene expression system in *Pseudomonas putida* KT2440. *Sci. Rep.,* 11(1):18079.
86. Rhu, MH, Zhang, J, Toth, T, Khokhani, D, et al. (2020) Control of nitrogen fixation in bacteria that associate with cereals. *Nature Microbiol.*, 5:314-330.
87. Choi, YJ., et al. (2010) Novel, versatile, and tightly regulated expression system for *Escherichia coli* strains. *Appl. Environ. Microbiol.* 76(15):5058-5066.
88. Seo, SO, Schmidt-Dannert, C. (2019) Development of synthetic cumate-inducible gene expression system for *Bacillus*. *Appl. Environ. Microbiol.* 103:303-313.
89. Park, TS, Kim, SW, Lee, JH. (2017) Efficient transgene expression system using a cumate-inducible promoter and Cre-loxP recombination. *Asian-Australas J. Anim. Sci.* 30(6):886-892.

90. Li Y, Lin Z, Huang C, Zhang Y, et al. (2015) Metabolic engineering of *Escherichia coli* using CRISPR-Cas9 mediated genome editing. *Metabolic Engineering*, 31:13-21.
91. Wang, HH, Isaacs, FJ, Carr, PA, Sun, ZZ, et al. (2009) Programming cells by multiplex genome engineering and automated evolution. *Nature,* 460(7257):894-898.
92. Huang, C, Guo, L, Wang, J, Wang, N, et al. (2020) Efficient long fragment editing technique enables large-scale and scarless bacterial genome engineering. *Appl Microbiol Biotechnol,* 104(18): 7943-7956.
93. Natsch, A, Keel, C, Pfirter, HA, Haas, D, et al. (1994) Contribution of the Global Regulator Gene gacA to Persistence and Dissemination of *Pseudomonas fluorescens* Biocontrol Strain CHA0 introduced into Soil Microcosms. *Applied and Environ. Microbiol.*, 60(7): 2553-2560.
94. Iavicoli, A. Boutet, E, Buchala, A. Métraux, J. (2003) Induced systemic resistance in *Arabidopsis thaliana* in response to root inoculation with *Pseudomonas fluorescens CHA0. MPM*I 16(10): 851-858.
95. King, E O, Ward, MK, and Raney, DE. 1954. Two simple media for the demonstration of pyocyanin and fluorescein. *J. Lab. Clin. Med*. 44: 301.
96. Shahid, I, Han, J, Hardie, D, Baig, DN, et al. (2021) Profiling of antimicrobial metabolites of plant growth-promoting *Pseudomonas* spp. isolated from different plant hosts. *3 Biotech*, 11(2):48.
97. Slininger, PJ, Shea-Wilbur, MA. (1995) Liquid-culture pH, temperature, and carbon (not nitrogen) source regulate phenazine productivity of the take-all biocontrol agent *Pseudomonas fluorescens* 2-79. *Appl Microbiol Biotechnol,* 43:794-800.
98. Bock, LJ, Hind, CK, Sutton, JM, Wand, ME. (2018) Growth media and assay plate material can impact effectiveness of cationic biocides and antibiotics against different bacterial species. *Letters in Appl. Microbiol.*, 66: 368-377.
99. Garrod, LP, Waterworth, PM. (1969) Effect of medium composition on the apparent sensitivity of *Pseudomonas aeruginosa* to gentamicin. *J. Clin. Path.*, 22; 534-538.
100. Tilton, RC Lieberman, L, Gerlach, EH. (1973) Microdilution antibiotic susceptibility test: examination of certain variables. *Appl. Microbiol.,* 26(5):658-665.

101. Gifford, DR, Furió, V, Papkou, A, Vogwill, T, et al. (2018) Identifying and exploiting genes that potentiate the evolution of antibiotic resistance. *Nature Ecology & Evolution*, 2; 1033-1039.

102. Holmes, RK, Minshew, BH, Gould, IK, Sanford, JP. (1974) Resistance of *Pseudomonas aeruginosa* to gentamicin and related aminoglycosides. *Antimicrob. Agents Chemother.*, 6(3): 253-262.

103. Kantor, RJ, Norden, CW. (1977) In vitro activity of netilmicin, gentamicin, and amikacin. *Antimicrob. Agents Chemother.,* 11(1):126-131.

104. D'Amato, RF, Thornsberry, C, Baker, CN, Kirven, LA. (1975) Effect of calcium and magnesium ions on susceptibility of *Pseudomonas* species to tetracycline, gentamicin polymyxin B, and carbenicillin. *Antimicrob Agents Chemother.,* 7(5):596-600.

105. Ramos, JL, et al. (2002) Mechanisms of solvent tolerance in gram-negative bacteria. *Annu Rev Microbiol.* 56:743-768.

106. Allard, N, Garneau, D, Poulin-Laprade, D, Burrus, V, et al. (2015) A diaminopimelic acid auxotrophic *Escherichia coli* donor provides improved counterselection following intergeneric conjugation with actinomycetes. *Can J Microbiol.*, 61(8): 565-574.

107. Suzuki, T, Yasui, K. (2011) Plasmid artificial modification: a novel method for efficient DNA transfer into bacteria. *Methods Mol Biol.,* 765: 309-326.

108. Swingle, B, Zhongmend, B, Markel, E, Chambers, A, et al. (2010) Recombineering using RecTE from *Pseudomonas syringae*. *Appl. Environ. Microbiol.*, 76(15):4960-4968.

109. Aparicio, T, Nyerges, A, Martínez-García, E, de Lorenzo, V. (2020) High-efficiency multi-site genomic editing of *Pseudomonas putida* through thermoinducible ssDNA recombineering. *iScience*, 100946.

110. Kumar, P, Nagarajan, A, Uchil, PD. (2019) DNA transfection by electroporation. *Cold Spring Harb Protoc.*, 7; 095471.

111. Silver, H, Siler-Khodr, T, Prihoda, TJ, Gibbs, RS. (1992) The effects of pH and osmolality on bacterial cell growth in amniotic fluid in a laboratory model. *Am J Perinatol,* 9(2); 69-74.

112. Court, DL, Sawitzke, JA, Thomason, LC. (2002) Genetic engineering using homologous recombination. *Annu. Rev. Genet*., 36:361-388.

113. Mosberg, JA, Lajoie, MJ, Church, GM. (2010). Lambda Red Recombineering in Escherichia coli Occurs Through a Fully Single-Stranded Intermediate. *Genetics*, 791-799, 186.

114. Thomason, LC, Constantino, N, Court, DL. (2016) Examining a DNA replication requirement for bacteriophage λ Red and Rac prophage RecET promoted recombination in *Escherichia coli*. *mBio*, 7(5):e01443-16.

115. Ellis, HM, Yu, D, DiTizio, T, Court, DL. (2001) High efficiency mutagenesis, repair, and engineering of chromosomal DNA using single-stranded oligonucleotides. *Proc Natl Acad Sci USA*, 98(12):6742-6746.

116. Filsinger, GT, Wannier, TM, Pedersen, FB, Lutz, ID, et al. (2020) Characterizing the portability of RecT-mediated oligonucleotide recombination. *BioRxiv*.

117. Wannier, TM, Nyerges, A, Kuchwara, HM, Church, GM. (2020) Improved bacterial recombineering by parallelized protein discovery. *PNAS,* 117(24):13689-13698.

118. Chang, Y, Wang, Q, Su, T, Qi, Q. (2019) The efficiency for recombineering is dependent on the source of the phage recombinase function unit. *BioRxiv*.

119. Pines G, Freed EF, Winkler JD, Gill RT. (2015) Bacterial recombineering: genome engineering via phage-based homologous recombination. *ACS Synth. Biol.*, 4:1176-1185.

120. Murphy KC. (2016) λ recombination and recombineering. *EcoSal Plus*.

121. Murphy, KC. (1991). Gam protein inhibits the helicase and stimulated recombination activities of Escherichia coli RecBCD enzyme. *J. Bacteriology*, 5808-5821.

122. Wannier TM, Ciaccia PN, Ellington AD, Filsinger GT, et al. (2021) Recombineering and MAGE. *Nat Rev Methods Primers*, 1:7.

123. Gurung D, Blumenthal RM. (2020) Distribution of RecBCD and AddAB recombination-associated genes among bacteria in 33 genera. *Microbiol.,* 166(11): 1047-1064.

124. Cox MM. (2007) Regulation of bacterial RecA protein function. *Critical Reviews in Biochemistry and Molecular Biol.*, 42:41-63.

125. Lajoie, MJ, Gregg, CJ, Mosberg, JA, Washington, GC, Church, GM. (2012) Manipulating replisome dynamics to enhance lambda Red-mediated multiplex engineering. *Nucleic Acids Res*., 40(22): e170.

126. Constantino N, Court DL. (2003) Enhanced levels of λ Red-mediated recombinants in mismatch repair mutants. *PNAS*, 100(26):15748-15753.

127. Mosberg, JA, Gregg, CJ, Lajoie, MJ, Wang, HH, Church, GM. (2012) Improving Lambda Red genome engineering in *Escherichia coli* via rational removal of endogenous nucleases. *PLoS One*, 7(9): e44638.

128. Lee DJ, Bingle LEH, Heurlier K, Pallen MJ, et al. (2009) Gene doctoring: a method for recombineering in laboratory and pathenogenic *Escherichia coli* strains. *BMC Microbiol.*, 9:252.

129. Binder S, Sielder S, Marienhagen J, Bott J, et al. (2013) Recombineering in *Corynebacterium glutamicum* combined with optical nanosensors: general strategy for fast producer strain generation. *Nucleic Acids Research*, 41(12): 6360–6369.

130. Aparicio T, Jensen SL, Nielsen AT, de Lorenzo V, et al. (2016) The Ssr protein (T1E_1405) from *Pseudomonas putida* DOT-T1E enables oligonucleotide-based recombineering in platform strain *P. putida* EM42. *Biotechnol. J.* 11(10):1309-1319.

131. Oh JH, van Pijikeren, JP. (2014) CRISPR-Cas9-assisted recombineering in *Lactobacillus reuteri*. *Nucleic Acids Research*, 42(17): e131.

132. Gallagher, R.R., Li, Z., Lewis, A.O., Isaacs, F.J. (2014) Rapid editing and evolution of bacterial genomes using libraries of synthetic DNA. *Nat Protoc*, 9(10):2301-2316.

133. Nyerges Á, Csörgó B, Nagy I, Bálint B, et al. (2016) A highly precise and portable genome engineering method allows comparison of mutational effects across bacterial species. *PNAS*, 113(9): 2502-2507.

134. Li, R, Shi, H, Zhao, X, Liu, X, et al. (2021) Development and application of an efficient recombineering system for *Burkholderia glumae* and *Burkholderia plantarii*. *Microb Biotechnol.*, 14(4):1809-1826.

135. Wang X, Zheng W, Zhou H, Tu Q, et al. (2022) Improved dsDNA recombineering enables versatile multiplex genome engineering of kilobase-scale sequences in diverse bacteria.

136. Gay, P, Le Coq, D, Steinmetz, M, Ferrari, E, et al. (1983) Cloning structural gene *sacB*, which codes for exoenzyme levansucrase of *Bacillus subtilis*: expression of the gene in *Escherichia coli*. *J Bacteriol*, 153(3):1424-1431.

137. Penewit K, Holmes EA, McLean K, Ren M, et al. (2018) Efficient and scalable precision genome engineering in *Staphylococcus aureus* through conditional recombineering and CRISPR/Cas9-mediated counterselection. *mBio*, 9(1): e00067-18.

138. Janick E, Niemcewicz M, Ceremuga M, Krzowski L, et al. (2020) Various aspects of a gene editing system—CRISPR-Cas9. *Int. J. Mol. Sci.*, 21(24):9604.

139. Ronda, C, Pedersen, LE, Sommer, MOA, Nielsen, AT. (2016) CRMAGE: CRISPR optimized MAGE recombineering. *Sci Rep*, 6:19452.

140. Wang Y, Liu Y, Liu J, Guo Y, et al. (2018) MACBETH: multiplex automated *Corynebacterium glutamicum* base editing method. *Metab. Eng.*, 47:200-210.

141. Lesic, B, Rahme, LG. (2008) Use of the lambda Red recombinase suite to rapidly generate mutants in *Pseudomonas aeruginosa*. *BMC Mol Biol,* 9:20.

142. Yin, J, Zheng, W, Gao, Y, Jiang, C, et al. (2019) Single-stranded DNA-binding protein and exogenous RecBCD inhibitors enhance phage-derived homologous recombination in *Pseudomonas*. *iScience*, 14:1-14.

143. Majumdar, C, Nuñez, NN, Raetz, AG, Khuu, C, et al. (2018) Cellular assays for studying the Fe-S cluster containing base excision repair glycosylase and homologs. *Methods Enzymol.* 599:69-99.

144. Jatsenko, T, Tover, A, Tegova, R, Kivisaar, M. (2009) Molecular characterization of Rif^r mutations in *Pseudomonas aeruginosa* and *Pseudomonas putida*. *Mutation Research*, 683:106-114.

145. Sharan, SK, Thomason, LC, Kuznetsov, SG, Court, DL. (2009) Recombineering: a homologous recombination-based method of genetic engineering. *Nature Protocols*, 4(2): 206-223.

146. Aparicio, T, de Lorenzo, V, Martinez-Garcia, E. (2019) CRISPR/Cas9-enhanced ssDNA recombineering for *Pseudomonas putida. Microb. Biotechnol.* 12(5):1076-1089.

147. Martinez-Garcia, E, Nikel, PI, Aparicio, T, and deLorenzo, V. (2014) Pseudomonas 2.0: genetic upgrading of *P. putida* KT2440 as an enhanced host for heterologous gene expression. *Microb Cell Fact,* 13: 159.

148. Aparicio T, Nyerges A, Nagy I, Pal C, et al. (2020) Mismatch repair hierarchy of *Pseudomonas putida* revealed by mutagenic ssDNA recombineering of the *pyrF* gene. *Environ. Microbiol.*, 22(1):45-58.

149. Anthony, JR, Anthony, LC, Nowroozi, F, Kwon, G, Newman, JD, Keasling, JD. (2009) Optimization of the mevalonate-based isoprenoid biosynthetic pathway in *Escherichia coli* for production of the anti-malarial drug precursor amorpha-4,11-diene. *Metab Eng*., 11: 13-19.

150. Zuker, M. (2003) Mfold web server for nucleic acid folding and hybridization prediction. *Nucleic Acids Res.* 31 (13), 3406-15.

151. Santa-Lucia, Jr (1998) A unified view of polymer, dumbbell, and oligonucleotide DNA nearest-neighbor thermodynamics. *Proc. Natl. Acad. Sci. USA* **95**, 1460-1465.

Appendix 1: Additional supporting data for Chapter 1

Table 1.1 Doubling times of *Pseudomonas* with different growth media

Strain	Media	Doubling time (hours)
P. chlororaphis 30-84	KB	2.79
P. chlororaphis 30-84	LB	1.44
P. ogarae F113	KB	1.75
P. ogarae F113	LB	1.74
P. fluorescens Pf0-1	KB	1.65
P. fluorescens Pf0-1	LB	1.89
P. protegens CHA0	KB	1.63
P. protegens CHA0	LB	1.43
P. protegens Pf-5	KB	1.71
P. protegens Pf-5	LB	1.25
P. synxantha 2-79	KB	4.48
P. synxantha 2-79	LB	3.23

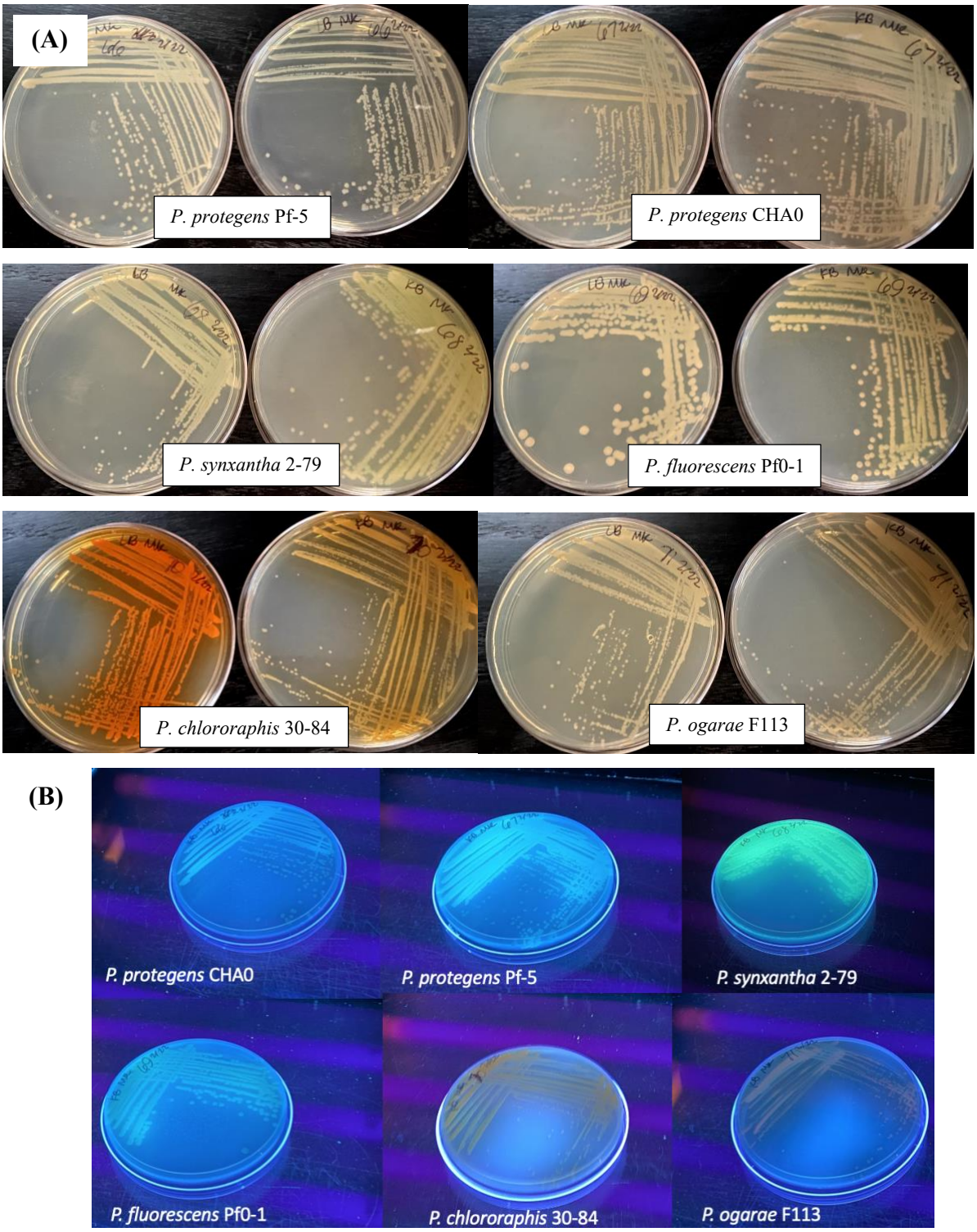

Figure 1.1 *Pseudomonas* on KB vs. LB. (A) Side by side comparison of pigment and siderophore production of strains grown on LB (left) and KB (right). Slight differences in phenotype can be observed. **(B)** Siderophore production observed under UV light when grown on KB.

Appendix 2: Additional supporting data for Chapter 2

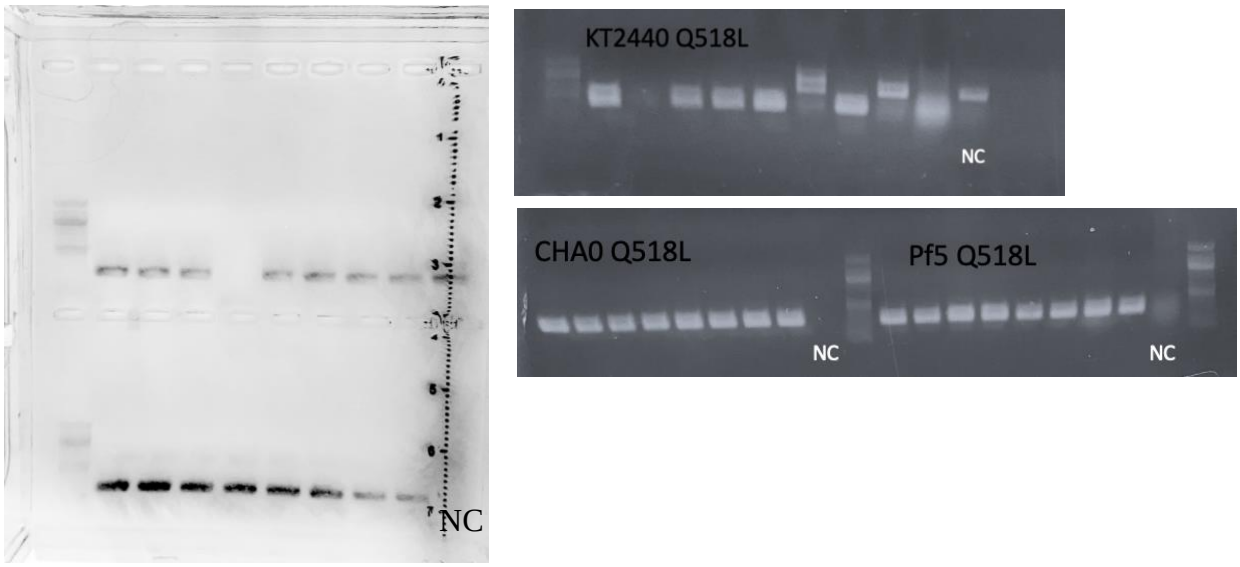

Figure 2.1 Mutation specific PCR for *rpoB* editing confirmation. (A) D521P confirmation in *P. protegens* Pf-5. **(B)** Q518L confirmation in *P. putida* KT2440. **(C)** Q518L confirmation in *P. protegens* CHA0 (left) and *P. protegens* Pf-5 (right) small, delayed growth colonies. All small colonies sequenced were found to carry the Q518L mutation.

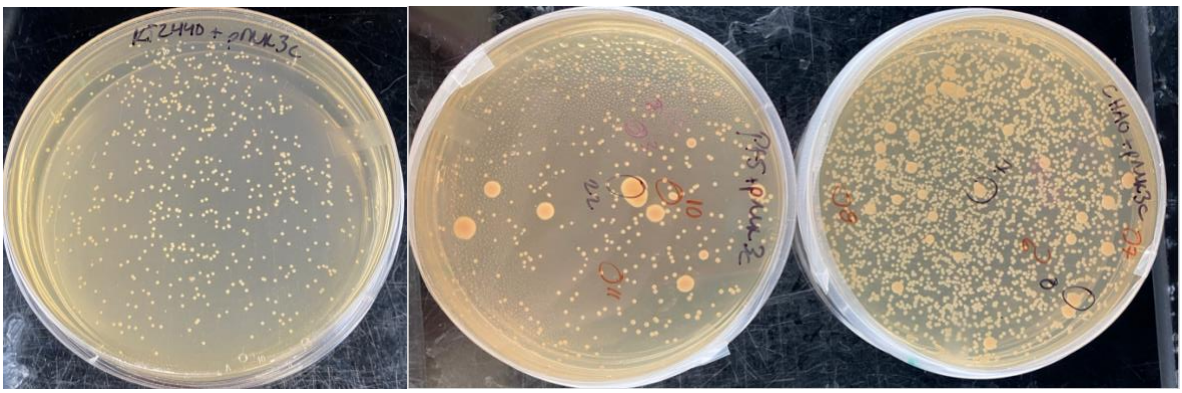

Figure 2.2 Delayed growth phenotype by Q518L mutation. *P. putida* KT2440 (left), *P. protegens* Pf-5 (center), *P. protegens* CHA0 (right) after recombineering experiment using the Q518L oligo. *P. putida* KT2440 + Q518L was imaged after two days of growth, after which no new colonies were observed, while the *P. protegens* strains were imaged after four days of growth, with the smaller colonies not being visible at 2 days of growth.

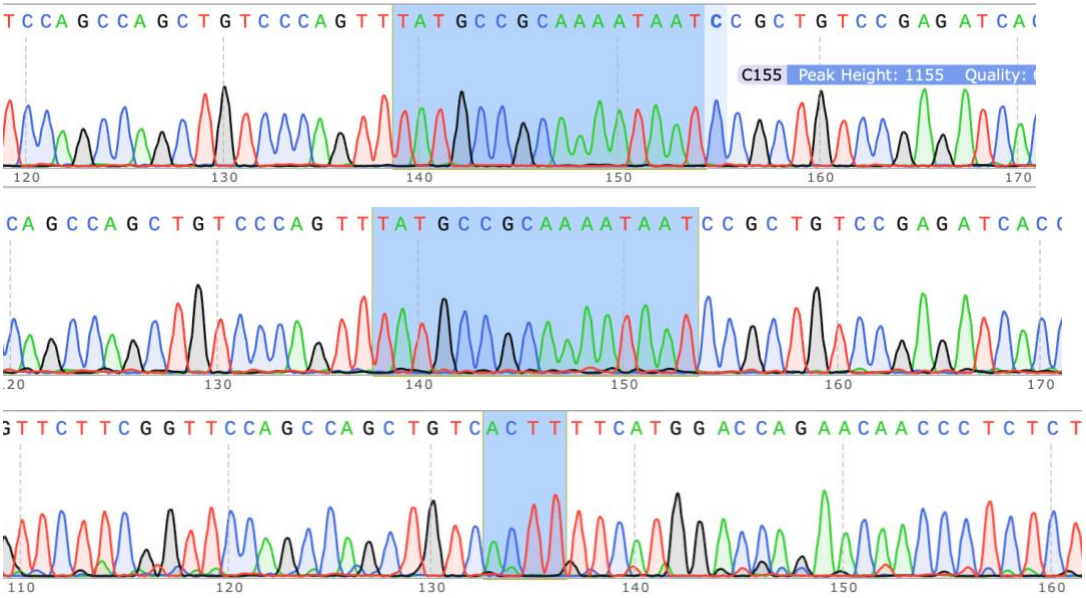

Figure 2.3 Presence of *rpoB* editing in *Pseudomonas*. Sanger sequencing chromatograms of the D521P mutation in **(A)** *P. protegens* Pf-5 and **(B)** *P. protegens* CHA0, or the Q518L mutation in **(C)** *P. putida* KT2440.